NYILATKOZAT

Név: Hetey Dániel

ELTE Természettudományi Kar, szak: Anyagtudomány MSc

NEPTUN azonosító: FGCN6U

Diplomamunka címe:
Emulsion Structures From Commercially Available Silica Nanopowders

A **diplomamunka** szerzőjeként fegyelmi felelősségem tudatában kijelentem, hogy a dolgozatom önálló szellemi alkotásom, abban a hivatkozások és idézések standard szabályait következetesen alkalmaztam, mások által írt részeket a megfelelő idézés nélkül nem használtam fel.

Budapest, 2022.12.07.

Hetey Dániel

a hallgató aláírása

Emulsion Structures From Commercially Available Silica Nanopowders

Thesis
Material Science MSc

HETEY DÁNIEL

Dr. Mészáros Róbert

Department of Physical Chemistry

Eötvös Loránd Tudományegyetem, Budapest
Faculty of Science
Institute of Chemistry
2023

Acknowledgements:

This work was supported by the Hungarian National Research, Development and Innovation Office under the NKFIH 137980 K project, which is greatly acknowledged.

I would like to express my gratefulness to my supervisor, Dr. Róbert Mészáros, for his continued support, scientific guidance, and our shared enthusiasm towards the project and research in general.

I owe thanks towards my laboratory colleagues, Mónika Bak and Anna Harsányi PhD students, Dr. Attila Kardos; Virág Anik and Levente Tulipán MSc students, and Kristina Sebestyén laboratory technician for the welcoming atmosphere, helpful advices and their efforts for maintaining the functionality of the laboratory.

Finally I would like to thank my family for all the support that allowed me to pursue higher education in the first place.

Table of Contents:

Introduction:

Material science has a very important role in our lives, as it enables us to manufacture products on an enormous scale, or with very special properties. It is the field of science that deepens our understanding of both the nanoscale interactions between components, and the possible, cost-effective, and tailorable ways of (mass)production of these materials.

In this study we chose to focus on emulsion based nanosystems with the hope of finding a well-reproducible and universal method to create special emulsion gels including, bijels as well. Bijel, is an acronym stands for Bicontinuous Interfacially Jammed Emulsion gels. These systems are particle-stabilized Pickering emulsion gels featuring two continuous immiscible phases, instead of the more common continuous and dispersed phase structure of common emulsions. Their existence has been predicted first in 2005 in a series of computer simulations performed by K. Stratford et. al.[1], two years later in 2007 E. M. Hertzig et. al.[2] confirmed this hypothesis through the first experimental synthesis of bijels using silica particles and a water-2,6-lutidine system[2]. There have been numerous suggestions for applications such as cross-flow microreactors[1-3,6,7], tissue scaffold templates[1-3,6,7], battery electrode templates[1-3], filter templates[1-3,6,7], etc.

Despite the promise they show as a new family of materials, their manufacturing is severely limited by the very strict criteria necessary for their production, holding their viability back. Our work focuses on the development of new production methods, which hopefully enable the large scale tailoring and manufacturing of these emulsions. Currently bijels can only be fabricated using neutrally with similar wetting affinity towards the immiscible liquid constituents of the emulsion [1-5] (Janus particles can be a great example for this[28]). This specific wetting feature of the particles can usually be achieved through expensive surface modification[2,3,4]. The other crucial and limiting requirement is that the mixture of the given liquid pair should have an appropriate phase diagram enabling spinodal decomposition (e.g.: water and 2,6-lutidine[2]) under practically accessible conditions. Furthermore, the structure of the bicontinuous channels that form in this process is outside of our control with only limited microscale tailorability[6]. The achievable macroscopic size for these bijels are also rather small because of the temperature quench based initiation of the spinodal demixing.

A few articles in the past have claimed to have been able to fabricate bijels in a top-down manner, by simply mixing two immiscible liquids[7,6]. However, years later, the current articles on bijels are still based on arrested bicontinuous structures formed upon spinodal

decomposition of specific liquid mixtures with no follow up publications about alternative methods.

The aim of our ongoing project is to conduct a systematic investigation of mixing-based emulsion fabrication possibilities with the ultimate goal of reproducible and tailorable bijel production. In this current study we are discussing some of our findings regarding the manipulation of emulsion phase inversions as one of the most promising alternative of spinodal decomposition for the development of a bicontinuous structure in an emulsion system.

Introduction to emulsions:

Emulsions are usually kinetically stable colloidal dispersions consisting of two (or more) immiscible phases; one of them is dispersed into droplets while the other one remains continuous. We can distinguish two main emulsion types based on which phase is the dispersed one. An emulsion that has oil droplets in water can be referred to as an oil-in-water emulsion (O/W), and if we have water droplets in a continuous oil phase that is a water-in-oil type emulsion (W/O). The use of water as a reference point is arbitrary, in the case of various polar and nonpolar immiscible phases the denotation remains the same. The type of an emulsion is an important parameter affecting various physico chemical properties including viscosity, conductivity, and stability of the system.[8,9]

Once an emulsion formed it has several ways to return to the equilibrium two phase state. The droplets can undergo creaming if the continuous phase is the denser one. The droplets can also sediment if they are denser than the continuous phase. In addition they can also flocculate, forming small clusters of discrete droplets in contact with each other. All of these processes only alter the position of the dispersed phase, and have no effect on the interfacial area of the system. Coalescence and Ostwald ripening are the two processes that can lower the contact area between the phases, thus lowering the interfacial energy of the system. Coalescence happens when two droplets of the same phase comes into contact and form a new larger droplet together. Ostwald ripening is the phenomenon when a smaller droplet is gradually dissolving into the continuous phase, and then condenses on the surface of a larger droplet. Ostwald ripening is caused by the curvature dependence of the chemical potential of the given component in the drops according to the Kelvin equation.[9]

In order to preserve the kinetic stability of the emulsion system and prevent the processes described above stabilizers are required[9]. The main categories of stabilizers are surfactants, polymers, and solid particles. These surface active materials adsorb onto the interface of the two immiscible liquids and lower the surface tension between them, decreasing the main thermodynamic driving force behind coalescence and phase separation. In the present work, particle and surfactant stabilizers will be used.

Surfactants are typical amphiphilic molecules usually with a hydrophilic “head” and one or more hydrophobic carbon chain “tails”. Many surfactants are able to self-assemble into monolayers or multilayers at various interfaces, or into different types of micelles. The residence time of the individual surfactant molecules in the adsorbed layers or in micelles is

relatively low, due to their small size and the low energy required to remove them from these assemblies. Micelles can also be formed by a mixture of surfactant species, which will have an effect on the properties[10].

Emulsions stabilized by solid particles are called as Pickering-Ramsden emulsions[25]. The adsorption energy of particles is usually larger, than that of surfactants due to their larger size covering more contact area between the immiscible phases. Their properties are also more easily tailorable by surface treatments or in-situ addition. Some of them can be made to be tens of nanometres in diameter as well as they can have different surface groups that modify their wettability. In addition the Pickering particles could have different shapes, or they can be coated by other materials[27].

One of the most important aspect of the kinetic stability of colloidal dispersions (including suspensions and emulsions as well) is related to the kinetics of flocculation and aggregation., which can be qualitatively predicted on the basis of the DLVO theory[9,26]. The main equation of the theory, written in a simplified form in *Equation 1*, describes the relationship between attractive and repulsive interaction (potential) energies acting between two approaching particles. *Figure 1* is a graphical representation of the theory in a general case. U_T (d) is the net potential energy, attractive or repulsive, acting on the particles in the function of d distance. U_{vdW} (d) is the sum of the van der Waals attractive forces; U_E (d) is the sum of double layer repulsive forces, as a function of d distance. U_{Born} (d) is a Born-repulsion term acting at distances that are less than the sum of the radii of the aggregated particles. This term originates from the repulsive forces between electron-electron and proton-proton pairs, and it prevents the model from allowing particles to occupy the same volume of space.

$$U_T(d) = U_{Born}(d) + U_{vdW}(d) + U_E(d) \qquad (\textit{Equation 1})$$

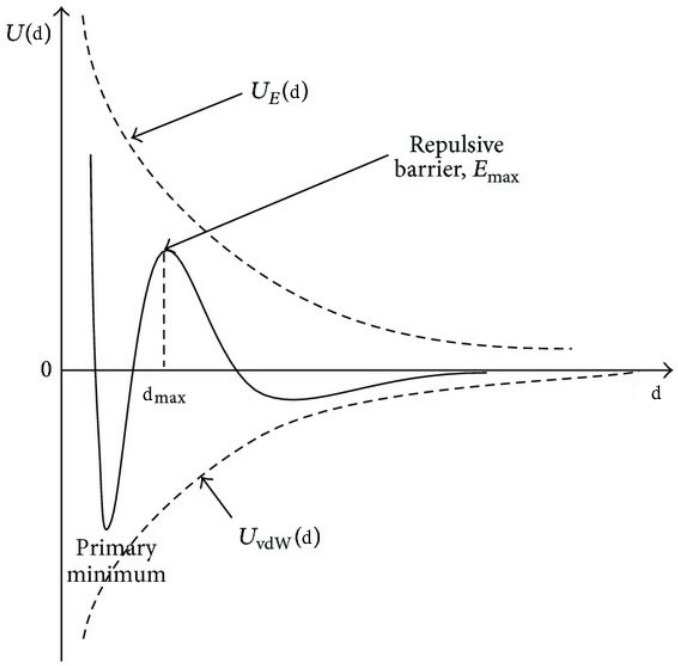

Figure 1: A schematic illustration of the DLVO theory[23]. The *r* distance between the particles is on the abscissa, and the *U* (*d*) energy is on the ordinate. U_E (*d*) is the net repulsion term, and U_{vdW} (*d*) is the sum of the attractive forces between the particles. E_{max} is the energy barrier between the reversible flocculation and the irreversible aggregation (secondary and primary minima), and d_{max} is the distance between particles where this barrier is the highestAt *r* distances less than the position of the primary minimum, the *U* (*d*) energy rises due to the U_{Born} (*d*) term.

Figure 1 shows that at infinitely large distances the interaction between the particles is nearly negligible, but they will attract each other more and more if they get closer. At some distance the U_T (*r*) function will have a local minimum called the secondary minimum, at which point the particles experience reversible flocculation. The flocculated particles are in loose clusters that can be broken up relatively easily because the net attractive forces acting between the particles are weak. Furthermore there is an E_{max} potential energy (a maximum net repulsion energy) at a specific d_{max} distance, which can be overcome only with sufficient kinetic energy of the particles to further decrease their distance. At the specific *d* distance corresponding to the primary minimum of U_T (*d*) the particles are irreversibly aggregating, and these tighter clusters can no longer be broken up without increasing the energy of the system through external means (e.g.: creating cavitations or other high energy mixing / dispersing techniques).

Pickering emulsions are stabilized by the layer of solid particles that form around the droplets, physically separating them from each other and preventing coalescence[12,29]. The

wettability of the particles at the liquid/liquid (L/L) interfaces is a very important parameter in the stability of Pickering emulsions[29]. This is characterized by the θ_{ab} contact angle, which is the angle between the L/L interface and the part of the particle that is submerged into one of the liquid phase[12,29]. A contact angle below 90° indicates favourable wetting of the particle for the given liquid. Therefore it will be the continuous phase and the interface will curve towards the other liquid phase, which will be distributed as droplets. The reverse is true when the $\theta_{ab} > 90°$, see *Figure 2*. A delicate situation arises when $\theta_{ab} = 90$, where there is net zero curvature in the system and there is no preference for the continuous or droplet phase It is important to note that wettability is strictly a surface phenomenon, which gives opportunities for it to be tuneable by surface treatments[8,25,12,29] (e.g.: impregnation on raincoats). During droplet coalescence the interfacial area of a system decreases, however for particle stabilized droplets this would require the removal of the solid particles, for which the energy needed is given in *Equation 2*.

$$-\Delta_{int}G = r^2 \cdot \pi \cdot \gamma_{ab} \cdot (1 \pm \cos\theta_{ab})^2 \qquad \textit{Equation 2}$$

$\Delta_{int}G$ is the change in interfacial free energy upon desorption of the particle, r is the radius of the particle, γ is the interfacial tension between "a" and "b" liquid phases, θ_{ab} is the contact angle. Specifically this expression gives the amount of work necessary for the desorption of particles from the L / L interface (particle/particle interaction in the adsorbed layer is neglected). Particles with a radius of 1000 nm need around 10^7 k_bT energy (at neutral wetting i.e. $\theta_{ab} = 90°$) for their desorption which is way above of what thermal motion can provide[7,12,29] .

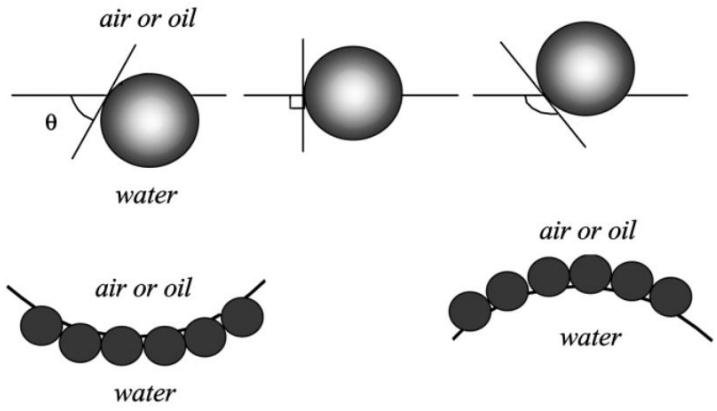

Figure 2: Illustration of liquid/particle/liquid contact angles and their imposed curvature on the interface. θ is the contact angle measured in water. This illustration belongs to B. P. Binks[12].

Stabilized emulsions can still adapt to changes in their environment or composition. One way for this is the phenomenon of phase inversion[12,30], in which the continuous phase will become the new dispersed phase, and the formerly dispersed phase will coalesce into forming the new continuous one. In this process the sign of the interfacial curvature in the system must change during the transition between the two states, i.e. the contact angle must go through $\theta_{ab} = 90°$ neutral wetting condition. The interfacial area is also possibly expanding during this process to some degree before shrinking back down again, thus this process has an activation energy requirement. There are two main types of phase inversion: catastrophic phase inversion (CPI), and transitional phase inversion (TPI)[12,30]. Catastrophic phase inversion is induced by increasing the volume fraction of the dispersed phase past a critical point ($\theta_{ab} = 90°$), where it will be more favourable for that phase to envelop the other. In the case of transitional phase inversion, the volumes of the two liquid phases are constant and the variation in the contact angle is the result of a change in factors such as the ratio of different stabilizers, or salinity, temperature, and possibly *in situ* surface modifications[12,13,30]

In the case of partially miscible phases, the phenomenon known as phase separation can take place[1-3,6,7,9]. If a previously homogeneous phase becomes thermodynamically unstable instead of just metastable, we talk about a spinodal phase separation. Spinodal phase separation (also known as spinodal decomposition) is a nucleation free process in a binary solution of solvents where they separate throughout the entire system simultaneously on a nanoscale. This is possible because in systems that exhibit this behaviour there is no thermodynamic barrier to the formation of a new phase, which can be triggered by infinitesimal fluctuations in temperature, pressure, or composition. In this case, non-equilibrium thermodynamics dictate the development of bicontinuous patterns in the beginning of the separation of the two liquid phase[9,11] as it can be demonstrated through the numerical solutions of the Cahn-Hilliard equation, which describes the change in the concentration of the given components in the domains formed during spinodal decomposition.

It should also be mentioned that arrested bicontinuous structures can form spontaneously in microemulsions[14,15]. Microemulsions are thermodynamically stable, optically clear and isotropic systems with surfactant stabilized droplets in the size range of 5 nm – 100 nm or with bicontinuous structure. They usually consist of two liquid phases, a surfactant, and a cosurfactant with extremely low L/L interfacial tension. The emulsion type can be O/W, W/O, or bicontinuous, and it is determined by the HLB (hydrophilic – lipophilic balance) of the surfactants. Therefore, in sharp contrast to bijels, the bicontinuous structure with net zero

interfacial curvature is not arrested but spontaneously develop if the hydrophilicity and lipophilicity of the amphiphilic small molecules is well balanced and the interfacial tension is extremely low. The microemulsion applications involve being used as template materials, self-microemulsifying drug delivery systems [S(M)EDDS][16]. They are also used in the creation of pesticides, personal care products, and cleaning agents. For our purposes however they are inadequate due to their very low surface tension, which does not support the adsorption of solid particles at the L/L interface.

In our present work we were synthetizing emulsion gel systems. Gels are soft-solids where a network forms wall-to-wall to solidify the otherwise liquid system[17]. This network can form from colloidal particles, polymer chains, surfactants, etc. and it possesses a yield stress. Emulsion gels are similar, however they contain two liquid phases in an emulsion structure. The two main types of emulsion gels are emulsion filled gels, and particle gels. An emulsion filled gel consists of a gel network, and the interstitial space is filled with the emulsion. A particle gel on the other hand, is built up from the droplets of the emulsion that form the gel network. In our work we are mainly discussing particle gels.

Bijel Literature:

The possibility of bijel formations was first proposed in 2005 by K. Stratford et.al.[1] According to their simulations, they predicted the existence of a kinetically arrested emulsion system where both phases are continuous, interpenetrating, and are stabilized by particles irreversibly adsorbed on the interface. In their publication they described the criteria necessary for bijel formation. The particles in the system need to be neutrally wetted by the immiscible phases i.e. the fluid-solid contact angle is near 90° in both liquids. This is required in order to achieve zero net curvature of the interface, and avoid the formation of droplets. The two phases need to be miscible in each other under certain conditions, usually at elevated temperatures, and be able to undergo spinodal phase separation when quenched.

The first bijel was created two years later in 2007 by E. M. Hertzig et. al. using the spinodal decomposition of 2,6-lutidine/water liquid mixtures and surface modified silica particles for neutral wetting[2]. They were able to confirm the bicontinuous structure in 3 dimensions spanning the entire sample using confocal microscopy. They found that the particle-laden interface was semi-permeable, which could enable their use for cross-flow[1-3,6,7]; phase transfer[1-3,6,7]; or micro reactor[1-3,6,7] applications. With high resolution imaging they were able to see that the structure was stabilized by a monolayer of particles held together by the interfacial tension and not by particle-particle interactions. They have tested the elasticity of the soft-solid bijel system by dropping a 1,9 mg cylindrical wire of 0,2 mm diameter onto a 2,6-lutidine-water critical composition bijel with 290 nm hydrodynamic diameter Stöber silica at a volume fraction of 2%. After they recorded its descent for some time, they have found that the wire easily sank in the non-bicontinuous reference sample, but was supported against gravity in the tortuous bijel indicating the existence of a yield stress for the structure. Furthermore, the structure was able to “regenerate” in a way that left no exposed liquid surfaces in the tunnel as a consequence of its deformation by the weight.

In 2015, D. Cai and P. S. Clegg managed to fabricate bijels using fumed silica nanopowders as opposed to the Stöber silica particles most articles reported using at the time[18]. Stöber silica particles are well-defined and monodisperse in size However, their wettability needs to tuned (which can serve as a liability in batch manufacturing) as well as they are also often contaminated by chemicals involved in their synthesis, water, ethanol, ammonia, which requires removal. Fumed silica particles on the other hand are available in a larger variety in terms of wettability (surface group composition) and are much cheaper. In exchange the

particles are much less uniform in their properties since they form secondary particle agglomerates (chains and clusters) in varying sizes and geometries.

In the mentioned work of D. Cai and P. S. Clegg mixtures of HDK® H30 silica particles (~ 50% silanol groups) with Aerosil® R972 (~ 31% silanol groups) particles and ethylene carbonate/p-xylene solvent mixtures were used to prepare bijels. Ethylene carbonate and p-xylene are partially miscible at higher temperatures, they used 100 °C, at a critical composition of 45:55 mol/mol. The silica mixtures dispersed in the single-fluid phase of ethylene carbonate and p-xylene, then a quenching induced spinodal phase separation which was arrested by the particles. This was the first time bijel fabrication could omit the lengthy and complicated surface treatment steps. The authors made the argument that the particles of the different silica powders possibly created new hetero-particle agglomerates which were able to stabilize the bijel To produce an arrested bicontinuous structure zero net curvature is required, which in principle can be achieved via neutral wetting for the Pickering particles. However, it is highly unlikely that all the hetero-particle aggregates wetted neutrally the L/L interface even if their wetting could be adjusted by changing the proportion of the H30 and R972 particles. It is more reasonable to assume that the hetero-agglomerates of the two different particles locally adjusted the curvature (to positive and negative values) resulting in a net zero curvature in the whole emulsion nanosystem. The hetero-particle theory was mentioned prior to their article by Binks and Lumdson[19].

Martin F. Haase et. al. in 2015 have worked out a continuous fabrication method for bijel fibers with a hierarchical structure[3]. They named this the STIPS method, an acronym for Solvent Transfer-Induced Phase Separation. (It works similarly to the DIPS method (diffusion-induced phase separation) that has industrial applications.) It uses a ternary liquid mixture (containing the partially miscible solvents in a common solvent and the stabilizing particles as well), and an external liquid phase (one of the partially miscible solvents), that can induce the diffusion of the common solvent. The ternary mixture is pumped in the inner capillary of a concentric capillary setup, and the external phase is pumped in the outer capillary. At the point where the inner capillary ends and the ternary mixture is exposed to the external phase, the common solvent starts to diffuse out of the ternary mixture causing the spinodal demixing of the partially miscible solvents. They used diethylphthalate and water as the bijel-forming phases, and ethanol as their common solvent. This ternary mixture contained 22 nm Ludox TMA nanosilica particles with cetyltrimethylammonium bromide surfactant for *in situ* surface modification (hydrophobization). The formed structures are the result of the

nonuniform mass transfer processes. Domain and pore sizes are usually larger in the inner sections where the arrest of the interface occurred later due to the relative depletion of the nanoparticles by that point in time. The time evolution of the arrested coarsening of the surface is also visible under microscope lengthwise. Depending on the flow rates in the two capillaries particles, segmented fibers or continuous fibers can be fabricated using this method. The preparation of two dimensional membranes based on STRIPS is also possible by dipping a glass slide first in the ternary mixture containing the particles and then into the solvent transfer phase[4]. The pores / channels structure can also be influenced by changing the surfactant concentration and the particle volume fraction. It should be also noted that in recent work of Vitantonio et. al., the STRIPS method was also successfully applied for the preparation of bijels using a mixture of hydrophobic and hydrophilic particles[20]. However, the major drawback of STRIPS is the requirement of specific ternary mixtures and no generalization and industrial scale-up is possible at the moment.

Huang et. al. in 2017 claimed to have been able to fabricate bijels in a way that did not require spinodal phase separation to occur in their article[3]. Instead, they simply emulsified two immiscible macroscopic liquid phases by vortex mixing. They were working with 16,5 nm acid-functionalized polystyrene (PS-COOH) nanoparticles dispersed in water, and amine-functionalized polydimethylsiloxane (PDMS-NH_2) in toluene. These components by themselves were not surface active, but the electrostatic interaction between them at the surface prompted the arrestment of the toluene-water interface. There were two distinct molecular weight versions of the PDMS-NH_2 polymer, namely a 1000 g / mol and a 3000 g / mol, which were used together to control the curvature imposed on the interface by the adsorbed particle-polymer layer. The 1000 g / mol molecular weight polymer alone created O/W/O or W/O type emulsions with the particles; whereas the 3000 g / mol molecular weight one only produced W/O emulsions. It is clear that the molecular weight of the polymer in this application has an effect on the curvature of the interface, thus they could be used in conjunction with the particles to create the near net zero curvature a bijel demands. According to their report, the molecular weights of the two polymers can vary in a wide range (1-10 kg / mol) as long as they are applied in the right mixture and concentration along with the solid particles to arrest a bicontinuous structure. They have managed to omit the spinodal decomposition from bijel fabrication by applying high shear rates to the immiscible phases and arresting the coalescence afterwards. They also reported that by altering the composition of the samples they could tailor the domain sizes of the arrested interpenetrating network

down to even only ~ 500 nm, which is one magnitude lower than what is commonly achievable via the spinodal route.

In the same year as Huang et. al., Cai et. al. have also worked out a method for bijel fabrication by simple mixing of two immiscible liquid phases[6]. They used HDK H2000 nanoparticles (14 nm in radius) from Wacker Chemie AG initially dispersed in ethanol, which was then added to glycerol as a sol. The ethanol was evaporated and CTAB surfactant was added to the dispersion. An immiscible silicone oil phase was added and this system was subjected to a slow mixing, followed by a fast mixing (with an optional pause in-between). (This is only a very short summary of their tedious procedure; details can be found in their publication[6].)

Seemingly these results represent a breakthrough and a promising alternative compared to the previously mentioned synthetic routes of bijel preparation based on arresting the spinodal phase separation via interfacial particle jamming. However, there are no general rules and protocols for bijel preparation via simple emulsification. For instance, in the case of the method published by Huang et. al.[7] numerous sophisticated components with arbitrary compositions are needed involving aqueous dispersions of functionalized particles and at least two functionalized polymers dissolved in oil. In the case of the second method published by Cai et al[6] three solvent and tedious, multistep protocol is necessary. Furthermore, up to our knowledge there are no follow-up publications of these papers and the current bijel applications still rely on the spinodal decomposition methods. We believe that the formation and locking of bicontinuous patterns in a heterogeneous system of two immiscible liquids is not a trivial matter and it needs to be further understood and generalized.

It should be mentioned that in 1976 an article was published discussing the theoretical possibility of creating a bicontinuous emulsion structure from a droplet lattice[21]. *Figure 3* shows the idea proposed in the paper: a cubic lattice of droplets, and thereby a cubic lattice of space between them can be transformed into two symmetrical and periodic, bicontinuous structure of truncated octahedra if partial coalescence occurs. This may result in a 15% decrease in the interfacial area of the system provided that the droplet volume fraction is around 0.5. They also mentioned that thermal fluctuation of the interface could destroy this structure on the scale of microemulsions, however we think that it could work for macroemulsions possessing larger domain sizes. This was ca. 20 years before the work of K. Stratford et. al. devising the idea of bijels.

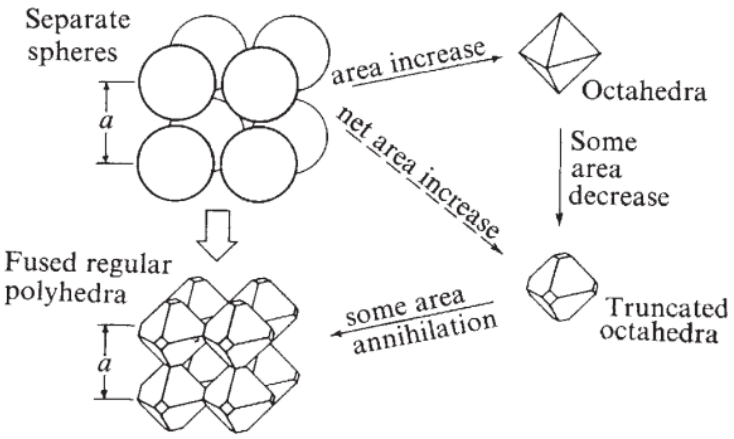

Figure 3: A schematic describing a theoretical process on transforming a cubic array of spherical droplets into a bicontinuous array of truncated octahedra. This illustration belongs to the corresponding article[21].

Our Goals:

The present production of bijels imposes many harsh limitations hindering their industrial application. Probably the most prominent issue is that the phase diagram of many commercially available, and environmentally friendly solvent pairs do not make the initiation of spinodal phase separation under practically relevant experimental conditions possible, which is the cornerstone of nearly every bijel preparation techniques as of today. The successful development of the bijel preparation methods based on simple mixing could be useful in analytics as well, creating chromatography columns with different liquids to alter the retention times of the species to be separated. Another benefit of not requiring spinodal phase separation would be the lifting of restrains in volume. In order to cause the demixing of a solvent pair a rapid change in temperature, quenching, is used most commonly. As we know currently, high cooling rates are only achievable in smaller volumes, or only in shallow depths near the surface of the sample; which greatly inhibits the creation of large sized, monolithic bijels due to the limited transfer of heat from greater depths. Of course, we are not ignorant of the difficulties experienced in the industry regarding the proper mixing of several hundred litre batch reactors either. A special sort of mixing, if the need arises, could be more troublesome for industrial applications, but it should be an easier task to carry out than the rapid cooling of larger batches.

In order to overcome the drawbacks of the earlier mentioned Huang[7] and Cai[6] methods, the basic hypothesis of the research was to utilize and tune the phase inversion of emulsions for bijel preparation. As we already discussed before, the 90 degree contact angle at the solid/liquid/liquid interface guarantee the net zero curvature. If one could understand the exact kinetics behind the formation and arrestment of a zero net curvature interface, it could in theory allow any two immiscible phases to achieve the same, at the cost of tweaking some parameters e.g.: viscosity, or surface tension; and the stabilization method of course.

Therefore, our primary aims were to deepen our understanding of phase inversions and to learn how to initiate one on demand.

In order to achieve our goals, we utilized cheap, commercially available silica nanopowder products with minimal if any surface modification. Another important motivation was to focus on the usage of environmentally friendly solvents such as isopropyl myristate, which is a frequently used constituent of cosmetic products.

We had performed different types of experiments to induce phase inversion. These can be divided into two groups such as:

i.) Mixing of hydrophilic and hydrophobic silica particles.

ii.) Manipulation of particle wetting via surfactant adsorption. A new approach was also applied based on the combination of nanoparticles dispersed in oil (and acquiring negative charge only at the water/oil interface) with aqueous solutions of the oppositely charged surfactant to tune the wettability of the particles and thus the emulsion type and phase inversion.

These studies have been performed simultaneously, in an attempt to develop a convenient method for bijel synthesis through simple mixing.

Materials:

Milli-Q water

We used ultra clean water from a Millipore Milli-Q Integral 3 water purification system. The treatment process done by the machine involves ion exchange, UV exposure, and 0,22 μm filtering just to name a few. This level of purity was needed because interfacial properties (e.g.: surface tension) are very sensitive to pollutants. The specific resistance of this purified water is around 18,2 MΩ / cm^2, the density is 0,9950 g / cm^3, viscosity of 0,890 mPa · s, and its refractive index is 1,333; all of these values were measured at 25 °C.

Isopropyl myristate

Our 98,4% pure isopropyl mysristate was acquired from Sigma-Aldrich, and was used as received. Isopropyl myristate is the ester of isopropyl alcohol and myristic acid. It is a widespread emollient agent in the cosmetics industry; it supports the skin absorption of products[24]. We used it as the apolar (oil) phase in our experiments with emulsions. Isopropyl myristate can be hydrolysed at higher temperatures to form alcohol and acid. *Figure 4* shows the structure of the molecule, and *Table 1* lists some of the more notable information related to isopropyl myristate.

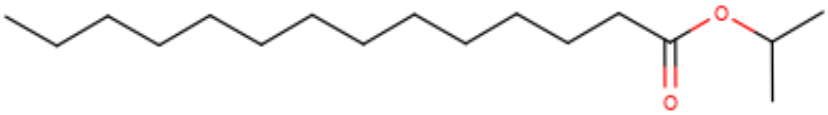

Figure Y2: The wireframe structure of an isopropyl myristate molecule with the hydrogen atoms not shown.

IUPAC Name	Propan-2-yl tetradecanoate
CAS number	110-27-0
Molecular weight	270,45 g / mol
Boiling point	588 K (315 °C)
Melting point	276,15 K (3 °C)
Vapour pressure	$9{,}35 \cdot 10^{-5}$ mm Hg (~ 0,0125 Pa)
Density*	0,8532 kg / m^3*
Viscosity	5-6 mPa · s
Refractive index	1,434
Water solubility	$2{,}44 \cdot 10^{-2}$ mg / L
Hazards	Irritant; Combustible; Toxic smoke / fumes

Table 1: This table shows some notable data about isopropyl myristate at 25 °C.
* This value was measured at 20 °C.

Toluene (Sigma-Aldrich)

We used 99,8% purity toluene from Sigma-Aldrich. Toluene is an aromatic, apolar and aprotic solvent with low water solubility. It has a relatively high vapour pressure of 28,4 mmHg at 25 °C (3,79 kPa). Being a benzene derivative it may be toxic to a lesser degree if inhaled, digested, or on skin contact. The molecular structure and main characteristics are found in *Figure 5* and *Table 2* respectively. Toluene was only used in a few instances for comparison to isopropyl myristate as a more apolar oil phase.

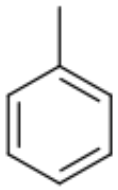

Figure 5: The wireframe structure of a toluene molecule with the hydrogen atoms not shown.

IUPAC Name	Toluene
CAS number	108-88-3
Molecular weight	92,14 g / mol
Boiling point	383,75 K (110,6 °C)
Melting point	178,25 K (-94,9 °C)
Vapour pressure	28,4 mm Hg (3,79 kPa)
Density	0,867 g / cm^3
Viscosity	0,560 mPa · s
Refractive index*	1,4967*
Water solubility	526 mg / L
Hazards	Irritant; Combustible; Target organ toxicity; Aspiration hazard; Reproductive toxicity

Table 2: This table shows some notable data about toluene at 25 °C.
* This value was measured at 20 °C.

HDK® N20 Pyrogenic Silica (Wacker Chemie)

HDK® N20 is a fumed silica powder that is hydrophilic. The manufacturer was Wacker Chemie AG., the product arrived in a 0,2 kg packaging and was used as received. It consists of amorphous colloidal aggregate particles that can be broken up by ultrasonic dispersing

methods. The N20 silica powder is frequently applied as thickening and thixotropic agent in coatings, inks, paints, and cosmetics; reinforcing fillers in elastomers; as well as it is also used in pharmaceutical products.

HDK® H30 Pyrogenic Silica (Wacker Chemie)

HDK® H30 is a hydrophobic colloidal silica powder produced by Wacker Chemie AG. Its surface groups contain ~50% -SiOH groups and ~50% dimethyl siloxane[18]. Its applications are similar to the ones mentioned for HDK® N20.

Cetyltrimethylammonium bromide (CTAB) (Sigma-Aldrich)

Cetyltrimethylammonium bromide, also known as hexadeyltrimethylammonium bromide (IUPAC name: N,N,N-Trimethylhexadecan-1-amonium bromide) is a quaternary ammonium surfactant which we used to alter the wetting of HDK® N20 silica particles. Our CTAB was produced by Sigma-Aldrich, and was used as received. Its water solubility is 36,4 g / L at 20 °C and its molar mass is 364,45 g / mol. The critical micelle concentration (CMC) of CTAB was found to be 0,92 mM. The molecular structure is shown in *Figure 6*. CTAB can be used among others in gold nanoparticle synthesis; as template for mesoporous materials; DNA extraction; and *in vitro* isolation of macromolecules inside cells.

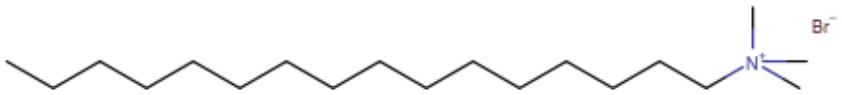

Figure 6: The wireframe structure of a CTAB surfactant molecule with the hydrogen atoms not shown.

Measurement methods:

Dynamic Light Scattering

To estimate the particle sizes and their polydispersity the method of Dynamic Light Scattering (DLS) was used, which is a fast, simple, and widely used process to characterize particles, polyelectrolytes, or polymers in solutions. In the laboratory we have used a Brookhaven made light scattering instrument capable both static and dynamic light scattering measurements. The instrument used a Coherent® Genesis MX488-1000 OPS laser (1 W) with a 488 nm wavelength, a BI-200SM goniometer, and a BI-9000AT digital correlator. The two detectors were both photoelectron multiplier tubes (PMT). The detectors were at a 90° detection angle, and the number of detected photons was kept between 50 kcps and 200 kcps to detect enough photons for the measurement without damaging the detectors. This setup was installed on a Standa Opto-Mechanics table to insulate it from vibrations. The scattering chamber was filled with decalin to compensate for the refractive index of the sample holder. The decalin was kept at 25 ± 0,1 °C using a Thermo Haake® C35P refrigerated circulator with a Phoenix II controller.

In DLS, due to the Brownian motion of the scattering centres the intensity of the scattered light also changes in time at a given scattering angle. If the intensity fluctuation is only caused by the unhindered Brownian motion (i.e. the contributions from rotations and interactions between the scattering centres is negligible), than the D_t translational diffusion coefficient in principle, can be determined, which proportional to the d_h hydrodynamic diameter of sphere-like particles according to the Stokes-Einstein equation, *Equation 7* However, it should be noted, that the above mentioned assumptions are only valid for well-defined particles with spherical shape and narrow size distributions.

The time dependence of the intensity of the scattered light is measured to record the $g_2(q, \tau)$ intensity-intensity autocorrelation function, which is then transformed using the Siegert-equation, *Equation 3*, into the electric field-electric field autocorrelation function $g_1(q, \tau)$.

$$\frac{g_2(q,\tau)-B}{B} = \beta|g_1(q,\tau)|^2 \qquad \textit{Equation 3}$$

where B is the experimentally determined baseline; β is a constant ($0 < \beta < 1$); q is the scattering vector; and τ is the correlation time. The absolute value of the q scattering vector is described by *Equation 4*.

$$|q| = \frac{4\pi n}{\lambda} \sin\frac{\theta}{2} \qquad \textit{Equation 4}$$

where n is the refractive index of the medium; λ is the wavelength of the incident light; and θ is the scattering angle. If the particle system is polydisperse, then the electric field - electric field autocorrelation function can be written as *Equation 5*.

$$g_1(q,\tau) = \int_0^\infty G(q,\tau)\exp(-\Gamma\tau)d\Gamma \qquad \textit{Equation 5}$$

where Γ is the relaxation time; and $G(q, \tau)$ is the relaxation time distribution. In the second order cumulant analysis method we can get the $\bar{\Gamma}$ average relaxation time and polydispersity without prior knowledge about the $G(q, \tau)$ relaxation time distribution, assuming monomodal size distribution. From the $\bar{\Gamma}$ average relaxation time we can get the $D_{app}(q)$ apparent diffusion coefficient as *Equation 6* shows.

$$D_{\text{app}}(q) = \frac{\bar{\Gamma}(q)}{q^2} \qquad \textit{Equation 6}$$

From here we can use the Stokes-Einstein equation, *Equation 7*, to estimate the $\bar{d}_{\text{h}}$ mean hydrodynamic diameter of our particles at the q value corresponding to 90° scattering angle.

$$D_0 = \frac{k_B T}{3\pi\eta\bar{d}_h} \qquad \textit{Equation 7}$$

where k_B is the Boltzmann constant; T is the thermodynamic temperature; η is the viscosity of the medium; and $\bar{d}_{\text{h}}$ is the mean hydrodynamic diameter.

Electrophoretic Mobility

We have used a Malvern Panalytical Zetasizer NanoZ tabletop electrophoretic mobility instrument with single-use DTS1070 measuring cells. Each measurement cycle consisted of a set of three, each of which was the average of 20 discrete measurements. All samples were measured at 25 °C. We have performed experiments, where we examined the effect of a cationic surfactant on the surface of negatively charged silica particles, and measured the electrophoretic mobility of the resultant particles. The process consisted of adding the known amount and concentration of CTAB solution to a silica sol during magnetic stirring at high rpm to ensure fast thorough mixing. I have waited for 15 to 20 seconds after addition to let the

components mix, then using a needle and syringe I transferred some of the sample into the measuring cell of the electrophoretic mobility measuring instrument. The measurements had to be carried out quickly after the mixing step, as both the wall of the 4 ml glass sample holder, and measuring cell were causing a continuous loss in CTAB surfactant in the system due to competitive adsorption processes. After the measurements were done, the measuring cell, syringe, needle, and magnetic stirrer bar were thoroughly washed to avoid cross-contamination between consequent samples.

This instrument also uses scattered light, but the theory behind the measurement is based on the electrophoretic movement of charged particles under the influence of an external electric field. *Equation 8* describes this relation.

$$u_\zeta = \frac{v}{E} \qquad \textit{Equation 8}$$

where u_ζ is the electrophoretic mobility; v is the velocity of the particle in the medium; and E is the strength of the applied external electric field. The instrument uses the M3-PALS method to calculate the velocity of the particles based on the phase difference between the scattered light that experienced a Doppler shift and a reference light. The Henry equation, *Equation 9*, is applicable for rigid, spherical particles, and it describes the relation between the u_ζ electrophoretic mobility and the ζ electrokinetic potential.

$$u_\zeta = \frac{\zeta \varepsilon_0 \varepsilon_r}{1{,}5\eta} f(\kappa\alpha) \qquad \textit{Equation 9}$$

where ε_0 is the permittivity of vacuum; ε_r is the relative permittivity of the medium; η is the viscosity of the medium; f is the Henry function; κ is the ionic strength; and α is the radius of the particles.

Optical Microscopy

Visual examination of the emulsion samples was carried out with a Reichert Austria Nr. 258 257 binocular optical microscope equipped with a CMOS 3.0 color digital camera. An optical microscope creates a magnified image by manipulating visible light that has interacted with the sample, by a series of lenses. The Abbe diffraction limit, presented in *Equation 10*

describes maximum possible resolution of microscopy techniques based on the wavelength of electromagnetic radiation used.

$$d = \frac{\lambda}{2n \cdot \sin\theta} = \frac{\lambda}{2NA} \qquad \textit{Equation 10}$$

where d is the smallest distance between two points where they are still visually separate (minimum resolvable distance); λ is the wavelength of the electromagnetic radiation interacting with the observed sample; n is the refractive index of the medium the electromagnetic radiation has to traverse; θ is the angle of the cone of focused light.

The main components of our microscope are a variable intensity light source illuminating the sample on the movable stage from below, the objective lens above it, the microscope camera and the eyepieces, and the computer connected to the camera with the compatible software for image processing.

Droplet Tests

Testing the emulsion type of our samples happened by looking at their miscibility in both pure water and pure oil phases separately. The emulsion sampling was carried out with single-use glass Pasteur pipettes two times from different regions of the samples. The containers for the pure liquids were emptied, washed, dried, and refilled between each test, and new clean containers were used to avoid contamination build-up. The results were always straightforward; miscibility was dependent on the continuous phase.

Additionally Sudan Red and Methylene Blue was added to confirm the result of the miscibility test in a few cases. Sudan Red has a very poor water solubility, while Methylene Blue is water soluble.

A drawback of these techniques however, is that they do not differentiate between O/W emulsions and W/O/W double emulsions. Optical microscopy evidence was needed for the identification of double emulsions.

Sample Preparation:

Weighing and Component Addition

We used a Mettler Toledo® AE 200 analytical scale to measure out the necessary amount of silica powder directly into our 4 ml glass sample holders. The scale was allowed around 30 minutes warm-up time after switching on and then it was calibrated with the built-in reference weight before the first measurement. I used a small laboratory spatula to handle the dry silica powders strictly under a fume hood at maximum performance! Samples were only taken out of the fume hood with their cap tightened on, and after being cleaned of floating silica with laboratory cotton wipes.

The liquid additions were carried out with Steinberg Systems SBS-PIP 100 automatic pipettes in the size range of 100-1000 µl. For smaller quantities Eppendorf Research® Plus single channel automatic pipettes were used that were precise in the 10-100 µl and 20-200 µl ranges.

For setting the basic pH we used 1 M NaOH solutions diluted with Milli-Q water. To set a pH of around 9,2 in a 1 ml aqueous suspension of either N20 or H30 we added 10 µl of 0,35 M NaOH solution after the first 15 seconds of ultrasonication. Due to the potential carbon dioxide absorption of NaOH solutions (and basic pH samples), all samples were prepared freshly and used right away.

Ultrasonic Dispersing:

The dispersing of our silica particles in their starting phase happened by ultrasonic dispersing. We used a Bandelin Sonopuls UW 3200 ultrasonic homogenator with a MS 72 sonotrode. The main components of the device are a user interface, wave generator, wave conductor, and the sonotrode. The wave generator uses a piezoelectric crystal to produce vibrations that are conducted and delivered to the sonotrode which creates cavitation with its fast movement. Cavitation is the phenomenon when vacuum bubbles are created momentarily in a liquid that is torn by strong shear forces. The homogenization / mixing happens as these vacuum bubbles collapse, generating very high local temperatures, a shockwave, and a strong jet of liquid. The sonotrode is made of a titanium superalloy, $TiAl_6V_4$ known for its high strength, because the generated liquid jets are usually aimed towards the solid surface that

caused the cavitation and these, along with the shockwave and temperature, can cause serious structural degradation. The MS 72 type sonotrode was chosen because its thin, relatively sharp head delivers the ultrasonic energy in a focused way.

An ice bath was used most of the time to counter the heat accumulation in the used liquids. This was most noticeable in isopropyl myristate, but the cooling was beneficial for aqueous sols as well. The dispersing process lasted for 1 minute for each sample at 20% power. This was enough to adequately break up larger particles and properly stir the suspension, but minimized the degradation of the ultrasonic tip, and excessive heating of the sol system.

Ultra-turrax emulsification:

For the emulsification of two immiscible liquids an Janke & Kunkel IKA-Labortechnik Ultra-turrax T25 homogenator (a non-digital version) was used with an S 25 N – 10 G dispensing tool. It has an electric motor that is connected to a mixing head (dispensing tool) that has a rotor-stator design. A rotor-stator design consists of rotating blades in close proximity of static ones, such as the compressor stage of a jet engine as an example. In our ultra-turrax homogenizator system we have two blades spinning inside a tube that has slits next to the blades. Forcing the liquids through these slits creates high shear forces that breaks the phases into droplets.

The emulsification of our samples was carried out for 1 minute at the maximum rpm of 25000, before and after there were about 5 seconds of wind-up and wind-down.

Experimental Work

N20 Dispersions in Water Phase

From our previous experiences with silica nanopowder products, we knew that the they arrive in a highly aggregated form, rather than as individual nanometre sized spheres. Thus, the work has started with dispersion experiments of N20, using the newly acquired silica product in ultrapure Milli-Q ion-exchanged water to create sol systems.. The resultant silica dispersions were then diluted, if it was deemed necessary, and the $\bar{d}_{\mathrm{h}}$ mean hydrodynamic diameter of the aggregate particles was estimated using Dynamic Light Scattering (DLS). N20 is a fairly hydrophilic particle and as a result it was simple to achieve a good level of dispersion.

The dispersed particles however were not of uniform size, nor shape, because of them being aggregates of nanoparticles, which were created by breaking up secondary aggregates of the nanopowder during ultrasonication. The question of filtration has occurred to us, and we have tried implementing it to our workflow, but we faced several problems. We choose single-use cellulose-acetate syringe filters with pore sizes of 0,45 μm. Cellulose-acetate was chosen due to its negatively charged surface in water preventing the attachment of the also negatively charged silica particles. The 0,45 μm pore size was selected in order to filter out larger silica aggregates, dust particles, and other contamination the sample might carry. This was supposed to be well within a comfortable margin of safety, as our DLS measurements have suggested, that the primary size range of particles is somewhere between 200 to 300 nm. However, whenever we tried filtering the dispersions, using a syringe and syringe filter, we always ended up with a water-clear filtrate, containing barely, if any, particles based on the DLS data. We are guessing, that the filtration process has exceeded a level of shearing stress, which caused our particles to quickly aggregate and block the syringe filter. This issue had not been resolved, so we investigated our samples without filtration similarly to the numerous studies of Binks[12,19,22] et al., Cleggs[6,18], and co-workers.

The as prepared 4 wt% N20 water sols were highly opalescent, therefore the turbidity had to be lowered by dilution to avoid, or at least minimize, multiple scattering during the DLS measurement. At 0,125 wt% N20 concentration, we could estimate a $\bar{d}_{\mathrm{h}}$ mean hydrodynamic diameter of about $\bar{d}_{\mathrm{h}}$ ~ 190 μm, with a polydispersity index of 0,18, at the pH the silica particles create themselves, pH ~ 4,2. At pH 9,2 these values have decreased to a $\bar{d}_{\mathrm{h}}$ average

hydrodynamic diameter of 150 nm and ~0,15 PDI, respectively. However due to the high polydispersity, we can assume that the degree of dispersibility of N20 in water is not dependent largely on the pH; at least in contrast to H30 particles with $\bar{d}_h$ > 1000 nm at pH 4,3 and $\bar{d}_h$ = ~ 250 nm at pH 9,1. This is a consequence of the favourable wetting with water and hydrophilic nature of N20 particles.

Our ability to disperse N20, and even H30, particles is better at basic pH conditions, but this at some point may be counterproductive. In order for particles to migrate to the liquid/liquid interface it is important that the electrostatic repulsive interactions between them are not too strong as to hinder their accumulation on the interface and the jamming effect.

N20 Dispersions in Oil Phase

In the present study we have investigated primarily isopropyl myristate and partly toluene as oil phases. Toluene was applied in a few cases for comparison but its toxicity and high rate of evaporation made it unfavourable for our purposes.

We have encountered a problem when trying to use DLS for the characterization of these dispersions. First of all, the scattering contrast was too small between the silica particles, with a refractive index of 1,46233 at 500 nm, and that of isopropyl myristate phase with a refractive index of 1,434 at the same wavelength at 20 °C. Furthermore, at higher silica concentrations the formed structured aggregated dispersions, prevented the estimation of the average hydrodynamic diameter.

The N20 silica particles dispersed in isopropyl myristate were closer to being measurable using DLS than in toluene. In *Figure 7* intensity-intensity autocorrelation functions are presented for particle dispersion in isopropyl myristate and toluene, respectively, as an example. The problem of secondary structure formation has caused fitting errors, but they are of a lesser magnitude than in toluene, and the estimated $\bar{d}_h$ average hydrodynamic diameters are consistently around several micrometres with high polydispersity. In toluene one could only argue qualitatively that large aggregates are present, which is also confirmed by the very high turbidity of these dispersions. The isopropyl myristate based N20 (and H30) sols appear as transparent, viscous liquids.

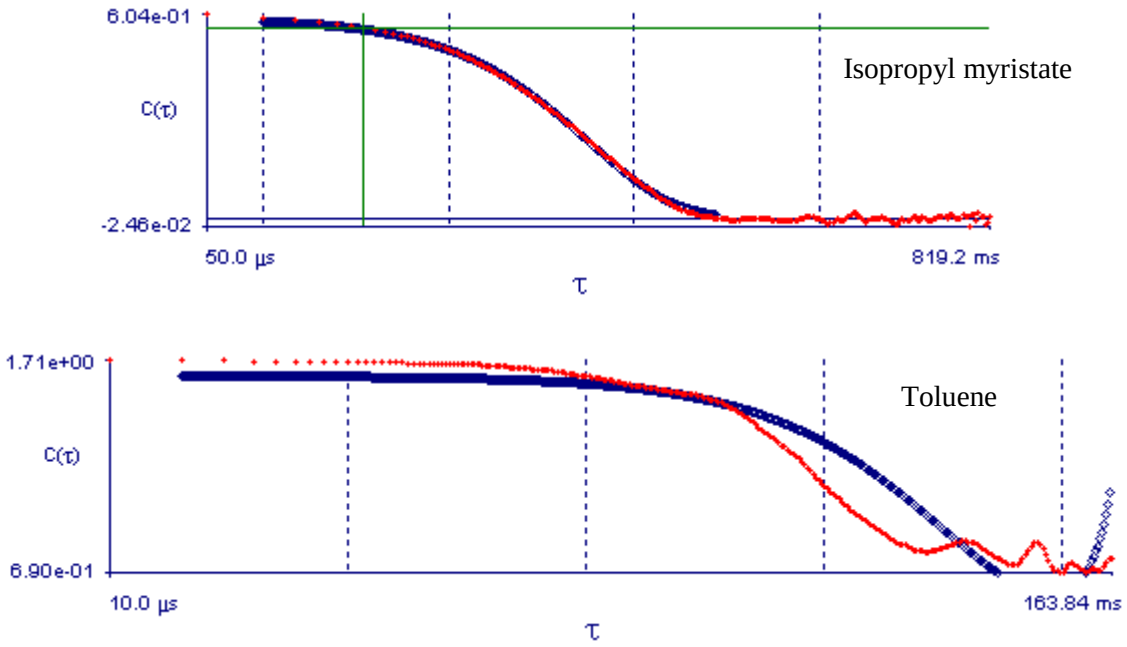

Figure 7: Screen captures of intensity-intensity autocorrelation functions measured for N20 particle dispersions, one in isopropyl myristate, and one in toluene. The red dots are the recorded points and the blue dots are the fitted function; τ denotes the delay time.

The possible reason, as to why the same nanopowder in ultrapure water creates particle agglomerates of 150-200 µm, but produces µm sized aggregates in isopropyl myristate, is likely due to the –SiOH silanol surface groups on the surface of particles as well as to the significantly higher viscosity and reduced polarity of isopropyl myristate compared to water. The -SiOH silanol functional group is a dissociable group in water, which is a protic medium, where it can protonate H_2O molecules, leaving behind a charge carrying $–SiO^-$ group, as it is presented in *Chem. Eq. 1* These SiO^- charged groups can cover the surface of the particles and create electrostatic repulsion between them. This serves to increase the E_{max} energy barrier, known from the DLVO theory [9], which prevents individual or reversibly flocculated particles from irreversibly aggregating. In an aprotic solvent however, the dissociation process does not take place. Therefore, it is likely that larger aggregates are formed in isopropyl myristate where the primary silica nanoparticles are hold together by hydrogen bonds.

$$R\text{-}SiOH + H_2O \rightarrow R\text{-}SiO^- + H_3O^+ \qquad \textit{Chem. Eq. 1}$$

N20 stabilized emulsions

The hydrophilic N20 and, to the some degree polar, isopropyl myristate produce some interesting results when they create emulsions with water. It was already a good result that 4 wt% of N20 powder could be dispersed in isopropyl myristate and not only in water, as it allows us more options to carry out experiments. We have observed that N20 has a preference to the water phase, thus it stabilizes O/W emulsions much more readily than W/O, but is possible. In light of this fact many of our experiments had the N20 particles first dispersed in isopropyl myristate, which forced the system to potentially undergo phase inversion when the particles migrate to be on the aqueous side of the interface. I say potentially, because it is possible that the particles reach their preferred position on the interface before any meaningful W/O emulsion structure could form during the initial stages of the mixing process.

It was observed with optical microscopy that N20 by itself can stabilize double emulsions with water droplets inside of oil droplets (W/O/W), see *Figure 8*. The water and the isopropyl myristate phases were in equal volumes with the particles initially dispersed in the oil phase. In principle, around the phase inversion a close to zero net curvature can be achieved in double emulsions as well. However in that case the droplet phases remain dispersed and disconnected instead of forming a bicontinuous interface. It does show however that N20 is promising candidate for our work.

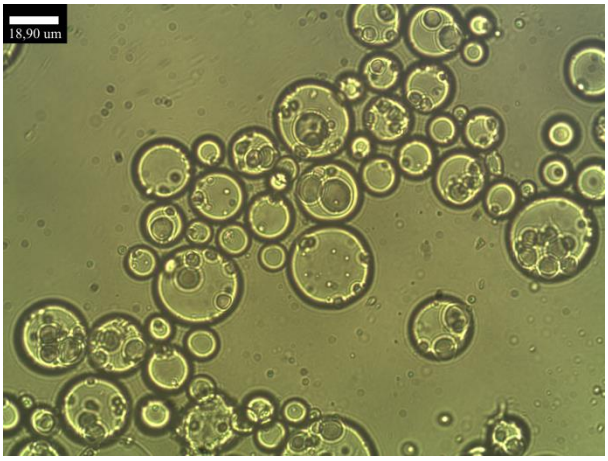

Figure 8: Microscopy image of an N20 stabilized W/O/W double emulsion in an isopropyl myristate – water system. The scale bar is 18,90 µm. The pH of the aqueous phase was set only by the N20 silica.

Other than the formation of double emulsions, another interesting phenomenon can occur. During microscopic imaging of an N20 stabilized isopropyl myristate – water emulsion I found a small part of the sample, that was not underneath the microscopy cover glass, and it had a seemingly continuous 3D structure as a result of minutes long ambient drying. It looked

as if many spatially separated channels were entangled between larger patches of isopropyl myristate. On *Figure 9* the parts that were protected by the cover glass and the parts that were exposed to air have visibly different structures. This new thin film structure has not yet been documented in the literature as far as we are aware.

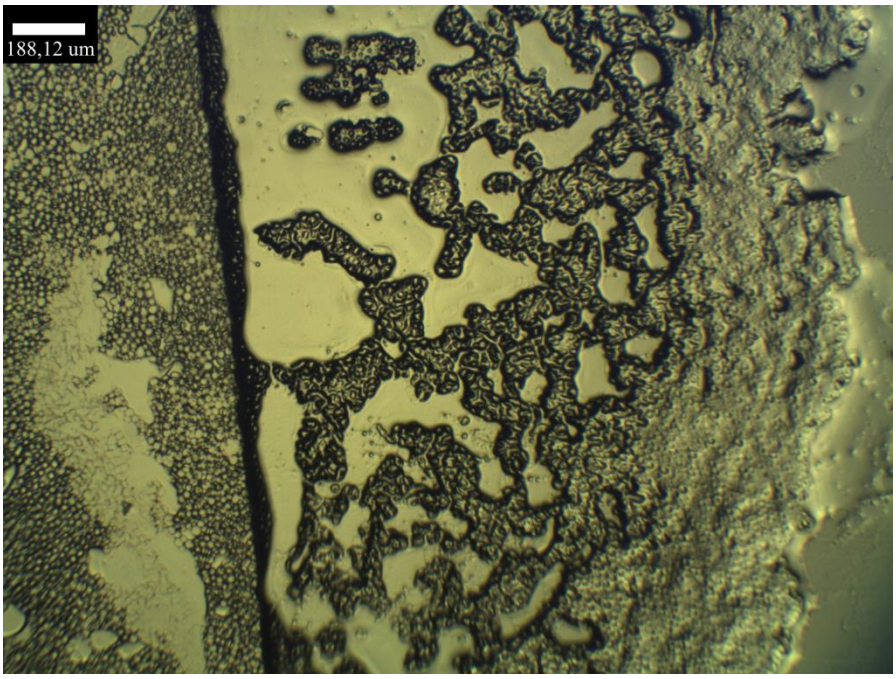

Figure 9: Micrograph of dried area of an N20 stabilized isopropyl myristate – water emulsion. We can see on the left the cover glass protected droplets; and on the right the area exposed to air. has formed a continuous and tortuous structure. The scale bar is 188,12 μm. The pH of the water phase was set only by the N20 silica.

We are hypothesising that the formation and arrestment of this structure could have been the result of a catastrophic phase inversion triggered by the evaporation of the continuous water phase. When the volume fraction of water decreases to a certain point by evaporation, the isopropyl myristate droplets may coalesce into more or less a single phase momentarily to encapsulate the remaining water in the form of discrete droplets. This process can be stopped if the N20 particles can arrest this unified isopropyl myristate phase by either interfacial jamming, or by increasing the viscosity of the medium through gelling.

This phenomenon was examined multiple times in order to gather more information. We managed to observe the transformation from the droplet structure to this entangled branch-like one, shown in *Figure 10 b*. A drying front sweeps through the uncovered parts of the microscopy sample at a rather high speed, it only needs a few seconds to cover the nearly 1 mm^2 area visible in the microscope. The droplets appear flattened, then they seemingly disappear with only their outline remaining faintly visible if anything, and then some time later some indentations appear and grow over time. The channels / branches start very thick

then slowly (minutes or hours) shrink until they reach their “final” size which they keep for weeks. On the freshly formed branches, the edges of former droplets are sometimes visible, confirming that the droplet phase (isopropyl myristate in our system) is the one forming this structure. It is important to mention that we could only see these kind of structures at 100x magnification; above that at 200x or 250x magnification we could only see patches resembling connected droplets (an example is provided on *Figure 10 h*).

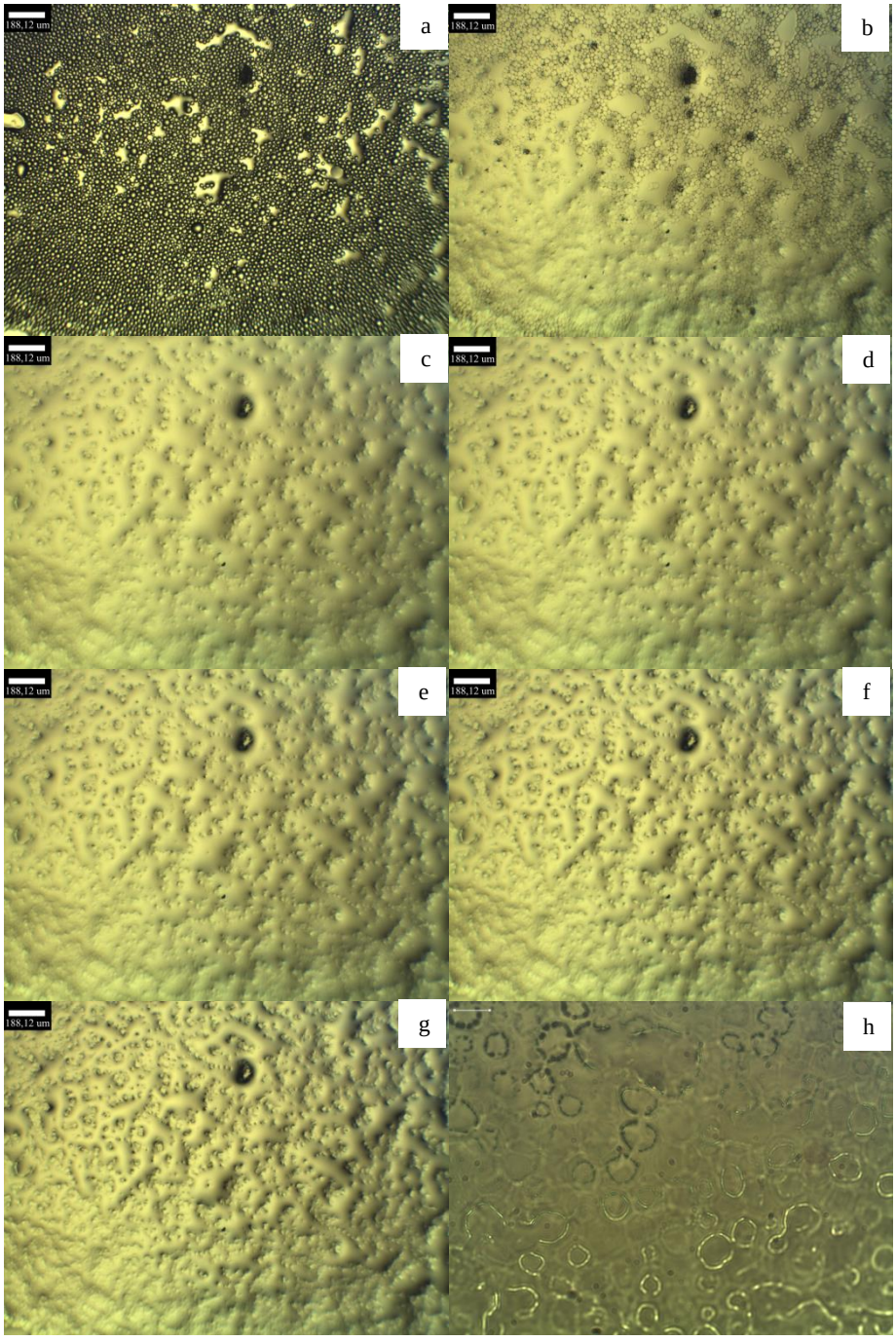

Figure 10: Micrograph series of a thin layer of N20 stabilized isopropyl myristate – water emulsion during drying. The pictures were taken at a) 0:00 (reference); b) 1:24; c) 2:04; d) 4:30; e) 6:44; f) 9:26; and g) 13:12 minutes of ambient drying. Pictures a) – g) are at 100x magnification; h) shows a picture taken at 630x magnification. The pH of the aqueous phase was only altered by the N20 silica.

Part of this sample has been placed under vacuum (~ 0,1 bar) for one hour in total to help the rapid evaporation of water from larger depths to se the forming network in a better developed state. The sample has been periodically examined under microscope. The result after 60 minutes in vacuum is presented in *Figure 11*. The characteristic size range for the branches is between 5 μm and 18 μm, for the opening of the pores it is between 12 μm to 30 μm. Keep in mind that the systems we are working with are not well defined and contain inhomogeneities, so the characteristic sizes may vary.

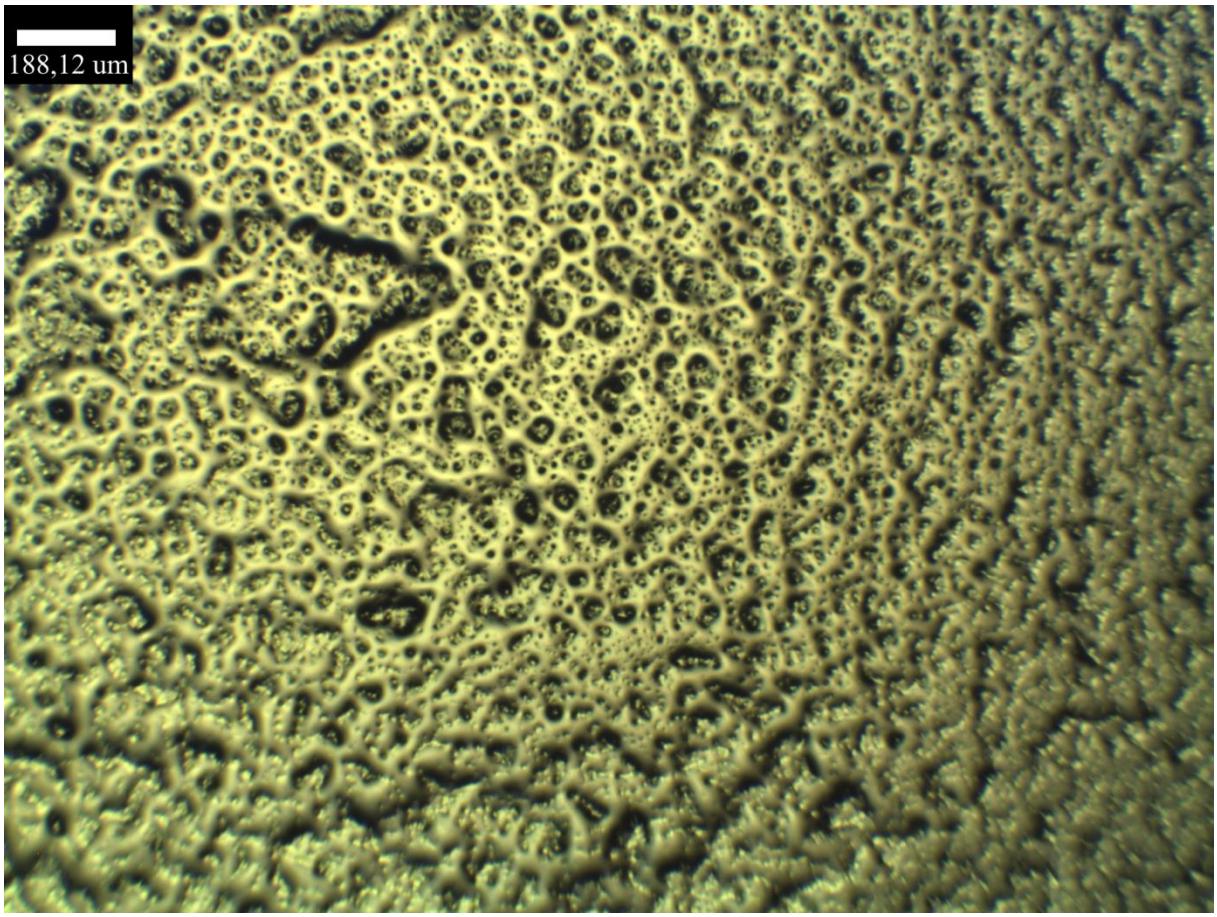

Figure 11: The vacuum dried thin film structure after 60 minutes. The emulsion contained 2 wt% N20 particles dispersed in the isopropyl myristate phase, and an equal volume of water. The pH of the aqueous phase was set only by the N20 silica.

Dispersing the N20 particles in both isopropyl myristate and water phases then mixing them together yielded other interesting structures. The formation of double emulsions did not occur; instead two regions are well distinguishable with different droplet densities on *Figure 12*. The mean droplet diameter in the darker domains is around 13 μm, in the lighter regions this is about 18 μm. It is likely that the darker regions originate from the water dispersed N20 particles, because the higher dispersibility in water would explain the higher number of droplets, and the lower droplet size average. This means that the migration of N20 particles

from the isopropyl myristate side to the aqueous side was incomplete after 1 minute of ultra-turrax mixing. The macroscopic stability for the emulsions synthesised this way is also lower, as usually a small amount of water separated within an hour after emulsification. The droplet tests suggest that O/W type emulsions have formed.

The structure of the area let to dry in ambient air; showed many droplets sitting on top of, or embedded in the continuous isopropyl myristate phase. *Figure 13* this structure.

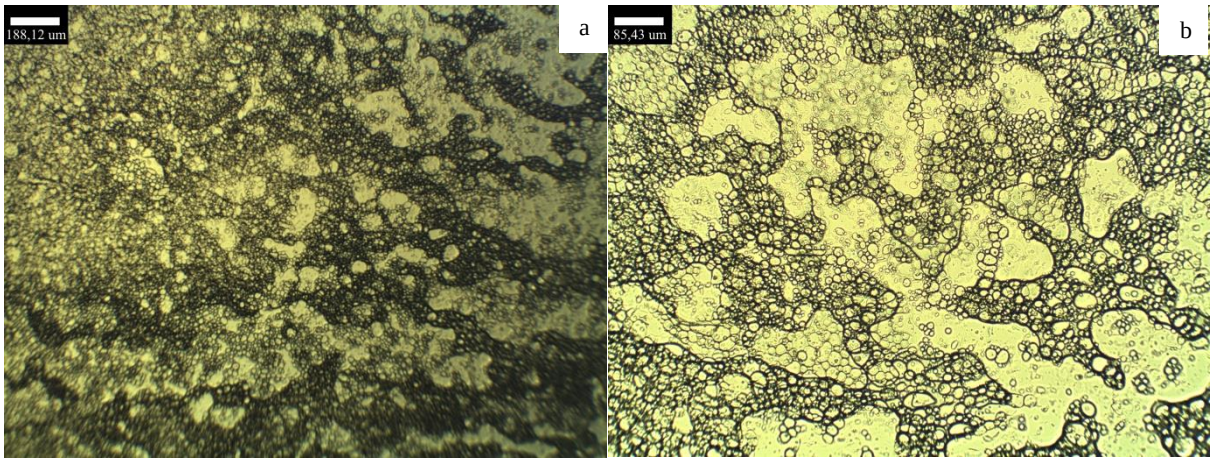

Figure 12: Micrographs of an emulsion containing 2 wt% N20 silica in both isopropyl myristate and water phases. The pH of the aqueous phase was set only by the N20 silica. a) and b) show two different droplet density regions at 100x and 250x magnification, respectively. The scale bars are 188,12 µm for image a), and 85,43 µm for image b).

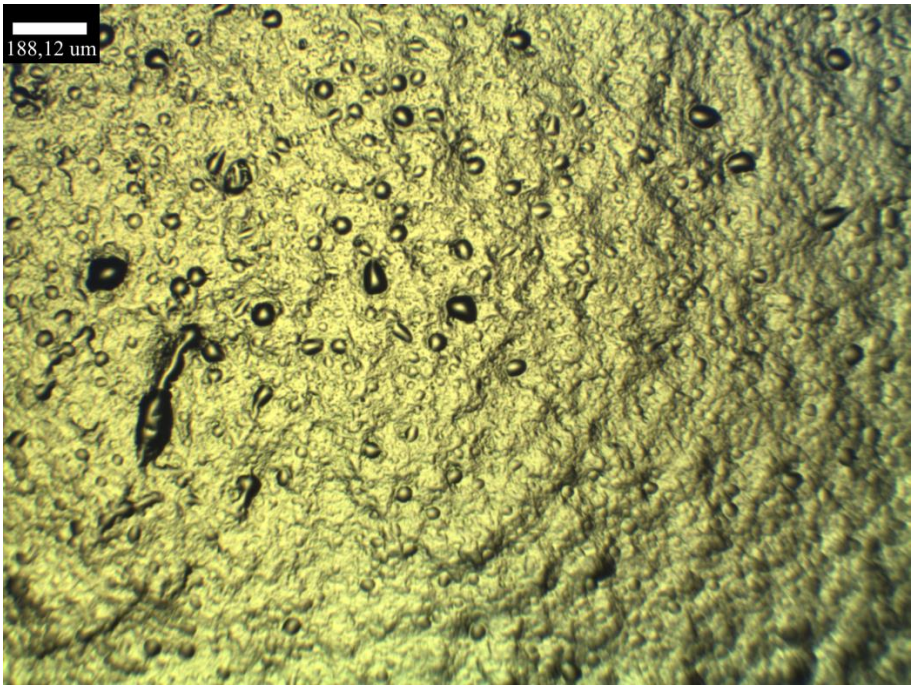

Figure 13: Micrograph of a dried area of an emulsion containing 2 wt% N20 silica in both isopropyl myristate and water phases. The pH of the aqueous phase was set only by the N20 silica. This image shows droplets on top of, or embedded in the particle stabilized rough surface of the sample. The scale bar is 188,12 µm.

H30 Dispersions in Water Phase

H30 is a semi-hydrophobic particle which can be dispersed in water, but it has a preference to more hydrophobic phases. Creating the aqueous dispersions is sometimes problematic, a significant portion of the silica powder can float on the surface of the water and it can take extensive shaking for it to submerge into the liquid. This can happen at both pH 4,3 and at pH 9,1. After the ultrasonic dispersing the sol system is more turbid than those made from N20, possibly indicating larger particle sizes. The suspensions have been diluted then measured using DLS.

At the pH set by the H30 silica (~4,3) the d_h average hydrodynamic diameter is over 1 μm with a polydispersity of around 0,23. If we set the pH to 9,1 the d_h average hydrodynamic diameter will be around 250 nm, although with a very large polydispersity of 0,18. The smaller particles can reach the interface more quickly than the larger ones, and at 250 nm the desorption energy from the interface is still magnitudes larger than the energy of thermal fluctuations, meaning that their interfacial attachment is irreversible. However, at pH 9,1 the electrostatic repulsion between them is increased considerably, with electrokinetic potentials of -15 mV at pH 4 and -35 mV at pH 9. This could hinder the self-assembly of an interfacial monolayer.

H30 Dispersions in Oil Phase

H30 was easily submerged in isopropyl myristate and in toluene. In both cases the viscosity has increased significantly even after ultrasonic dispersion it was noticeably higher. The sols were transparent, and thin films have stuck on the glass wall of the sample holders.

DLS measurements of oil dispersed H30 silica were not feasible due to gelation in both isopropyl myristate and toluene phases. Diluting the suspensions did not alleviate this problem, the particle concentration became too low for measurement before the structure formation would have been supressed. It is probably a good assumption that the particles were several micrometres in diameter, since the increased viscosity in these phases hindered the cavitation-induced effects of the dispersing process. The sample indeed had to be moved in a circular motion during the ultrasonication to keep the tip of the sonotrode in the viscous liquid.

H30 stabilized emulsions

H30 is more hydrophobic than N20, so it stabilizes W/O emulsions. The emulsions are similar in appearance to the N20 stabilized ones, they are white and do not flow until shaken. Their stability was low with some water separating shortly after emulsification. Under the microscope we saw a large number of dark blurs which were presumably large H30 silica aggregates, which were not present in N20 stabilized emulsions, examples can be seen on *Figures 14* and *16*. The number of droplets was also much lower, and their shape was irregular. These silica patches were present regardless of which phase were the particles dispersed in, but they were more prevalent in isopropyl dispersed cases.

Controlling the Interfacial Curvature Through Silica Mixture Composition

Huang et. al. claim to have induced the formation of bijel structures via simple mixing of two macroscopic immiscible phases[7]. Our goal was similar, namely, to control the interfacial curvature between the two liquid phases via the composition of the mixtures of silica samples. If we could create an interfacial film of a particle blend, where each particle would counteract the curvature formation of the other, then a film of that sort, in principle, would be able to fulfil the zero net curvature requirement of bijel formation. This method also has the possible benefit of not requiring expensive, long, or complicated surface modification steps as for example the creation of Janus-particles usually require[28]. The inexpensive nature of this method could also enable the large scale industrial manufacturing of these bijels for their claimed applications[18] mentioned in the beginning of this thesis. In fact, Cai et. al. have already reported the usage of blends of particles with different hydrophilicity for bijel preparation[18], however they were relying on spinodal decomposition, and used in ethylene carbonate and p-xylene containing systems.

HDK® N20 and H30 are relatively cheap, commercially available silica nanoparticles that by themselves do are not neutrally wetted by water and isopropyl myristate. H30 is possibly an in-between of hydrophobicity and hydrophilicity; and N20 is a mostly hydrophilic silica. Theoretically the proper combination of these two could act as a replacement for a well-defined, neutrally wetted particle, at a fraction of the cost.

The volume ratio of water-to-oil was kept at 1:1 due to some of our previous results indicating that emulsion systems that largely deviate from this phase ratio are usually low in stability. Articles dealing with transitional phase inversion and emulsions in general also often work with 1:1 phase ratios or just slight alterations to it[1-3,6,7].

We made samples with H30 and N20 fumed silica particles with H30 acting as the more hydrophobic and N20 as the hydrophilic particle. These silica particles (2 wt% in total) have been dispersed in isopropyl myristate and only during emulsification could the first interactions occur between the particles and the aqueous phase. This was decided on because phase inversion can only happen when an emulsion system changes from a less stable to a more stable state[9,19]. As most of our emulsions using N20 were of the O/W type, it was clear that it has a wettability preference towards the water, and H30 has a semi-hydrophilic wettability with possibly a preference towards hydrophobic phases. However N20, initially dispersed in isopropyl myristate, was capable of stabilizing double emulsions, meaning that its wettability is probably close to neutral by itself.

When the stabilizing particles in a 1:1 isopropyl myristate to water system consists of 100% N20 fumed silica particles, the samples will form O/W emulsions, or W/O/W double emulsions. The hydrophilic N20 particles cross the oil-water interface from the oil side, and will settle at a contact angle that is less than 90° in water. In the case of 100% H30 silica, the emulsion will be W/O with the particles only partially wetted by water, meaning a contact angle above 90° in water. These emulsion types have been confirmed by droplet testing.

For the 95% N20 and 5% H30 mixture, the emulsion droplets are miscible in water and float on isopropyl myristate, so the emulsion that formed is proposed to be O/W. Under the microscope, however the sample has a W/O appearance in some areas, with both wrinkles in the continuous phase and hazy, darker spots, likely aggregated silica, see *Figure 14*. This is an unusual sight for supposedly O/W type emulsion, but in other areas the sample does not show these characteristics. The usage of a Pasteur pipette can also change what we see under the microscope or in the droplet test based on sampling depth.

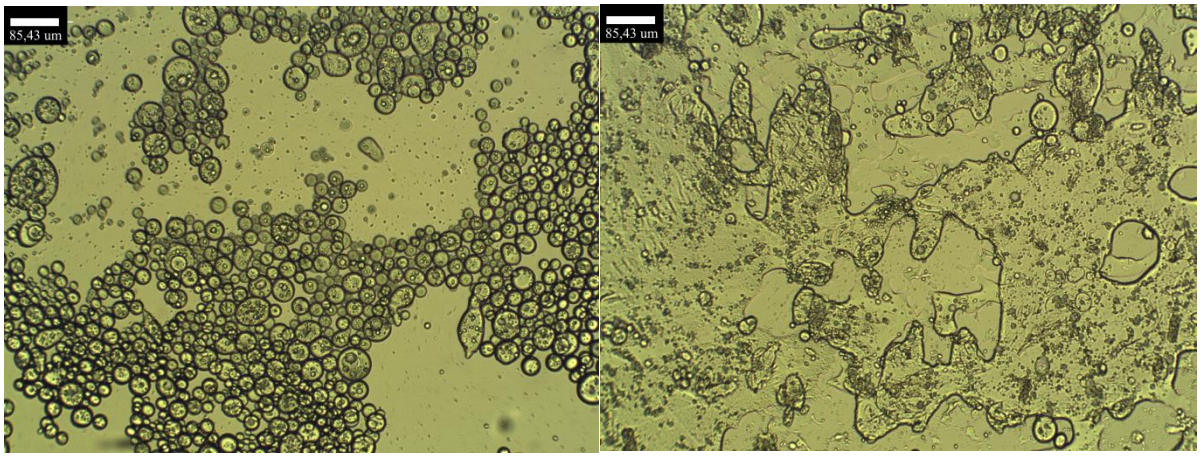

Figure 14: Micrographs of the 2 wt% (95% N20 – 5% H30) silica containing emulsion The particles were dispersed in isopropyl myristate, and the pH of the water phase was not set. We can observe both W/O/W and W/O regions within the same sample droplet. The scale bars are 85,43 μm.

The micrographs are also showing that the droplets (supposedly isopropyl myristate) contain droplets themselves (likely water). This is then a W/O/W double emulsion, based on the images and the result of the droplet test. This indicates several things. First, this means that system has two surface active components, the two types of silica particles, which are capable of stabilizing opposing interfacial curvatures, which leads to the formation of both oil and water droplets. This has been part of our hypothesis, described at the beginning of this section, and here we see some degree of confirmation. This can also mean that inhomogeneities in particle distribution can create areas that are richer in one silica type, which will determine the local structure and other properties. Second, the system is possibly near a transitional state, where the typical binary categorization of O/W and W/O emulsion types is no longer applicable perfectly, as the system fits into both simultaneously.

If we continue changing the silica mixture we can observe some changes in the microstructure. In general the droplet sizes decrease, while the droplet density increases as we increase the H30 content of the mixture. Something similar can be said about the non-mixed silica samples: the 100% N20 containing emulsion has relatively large oil droplets (average diameter ~ 14 μm), while the 100% H30 stabilized emulsion has much smaller water droplets (average diameter ~ 3 μm) packed very tightly. *Figure 15* shows this difference.

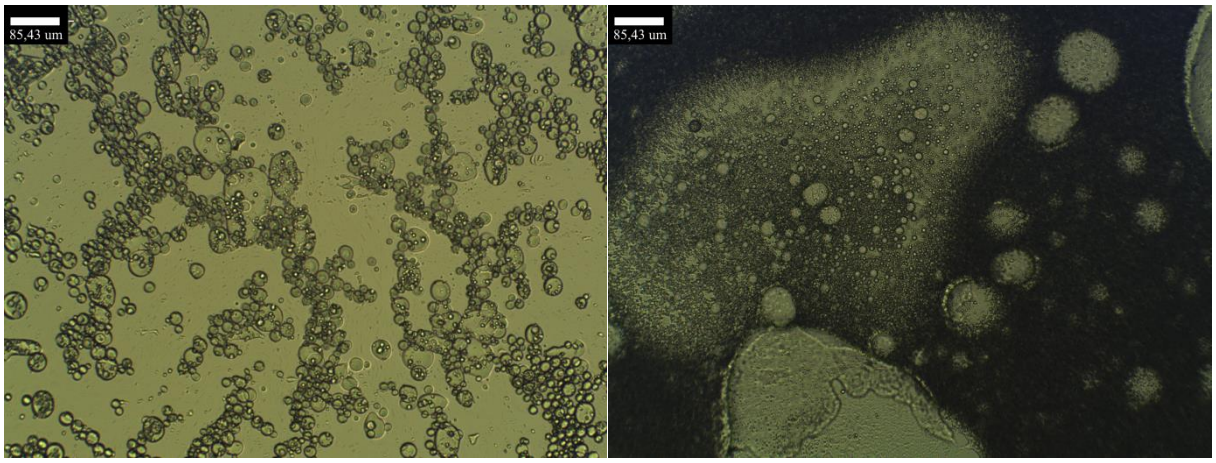

Figure 15: Micrographs of the 2 wt% N20 (left) and H30 (right) silica containing emulsions respectively. These two images show the differences in the droplet sizes based on the emulsion stabilizing particle. The N20 stabilized emulsion (left) is a W/O/W type, and the H30 stabilized (right) is a W/O type emulsion. The scale bars are 85,43 μm.

A mixture of 90% N20 and 10% H30 nanopowders can cause the formation of a W/O type emulsion. The sample will behave as a hard gel, and is not only capable of being flipped upside down for hours even; it can also maintain its shape after sample manipulation. For the droplet tests and in the preparation of microscopy samples, I have used single-use glass Pasteur pipettes, after which an emulsion sample such as this one could keep a fibre-like shape (inherited from the design of the Pasteur pipette).This fibre has an intermediate density, meaning that it floats on Milli-Q water, but sinks in isopropyl myristate, which is logical given that it consists of a mixture of the two phases. O/W emulsions always formed droplets; only W/O emulsions revealed this phenomenon. The exact reason behind this observation is unknown to us, but the viscosity of these samples must play a key role in this. It may be a consequence of H30 particles aggregating; possibly increasing the viscosity or forming a different gel structure. The micrographs of this sample show large clusters of aggregated silica, as seen on *Figure 16*.

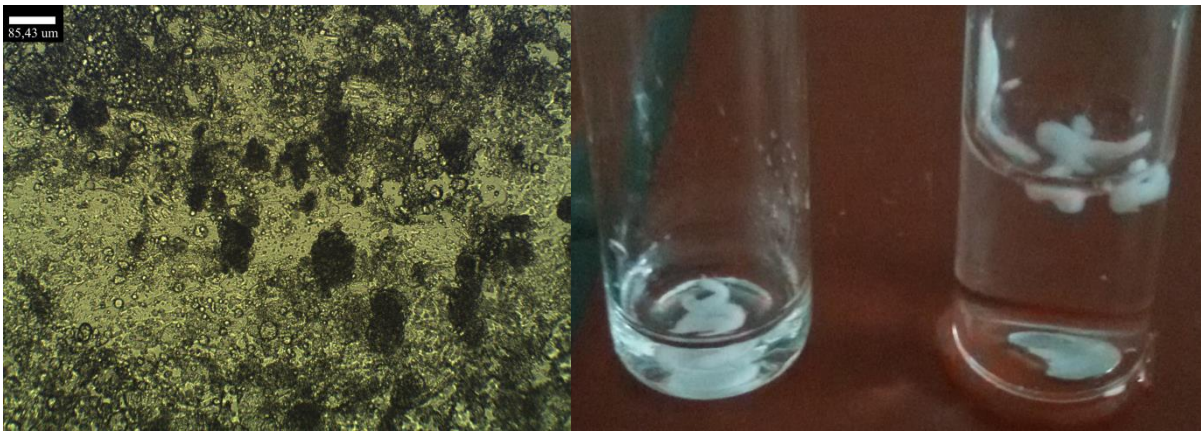

Figure 16: On the left: a micrograph of the 2 wt% (90% N20 – 10% H30) silica containing emulsion The particles were dispersed in isopropyl myristate, and the pH of the water phase was not set. Despite the O/W droplet test result, this sample looks more similar to a W/O emulsion due to the wrinkled continuous phase and the silica clusters. On the right: a photograph of the emulsion forming a "fiber" instead of a droplet when squeezed out of a Pasteur pipette. It did not mix with either of the phases on contact, but it did with isopropyl myristate when the container was shaken.

However, the resulting emulsion type with this silica mixture has a rather large uncertainty. If we repeat this experiment, we may find that the emulsion is an O/W type, and that it cannot be "extruded" into a fibre with a Pasteur pipette, it forms droplets instead. Some of these samples have been repeated multiple times in an attempt to counteract this apparent unpredictability.

80% N20 and 20% H30 stabilized a W/O emulsion, along with the other samples in the experiment with 60%-40%; 40%-60%; and 20%-80% N20-H30 particle ratios. However, the emulsion types were not reproducible at lower H30 amounts. For example once we made a set between 95% N20 and 80% N20 content, and all of them were O/W, when other experiments have indicated according to the drop tests that emulsions with 90%; 85%, and 80% N20 can be W/O.

Since the previously described experiments did show some viability, despite the uncertainty between 100% N20 and 80% N20 – 20% H30, we tried to disperse the different types of particles separately to see if it has any influence on the emulsion type. The dark spots in some of the other samples suggested that the dispersing of the silica mixture is incomplete, so we deemed dispersing them separately as a probable workaround of this issue. The silica mixture was chosen to be 80% N20 – 20% H30 because it was close to the region where the emulsions were unambiguously W/O (70% N20 – 30% H30 down to 100% H30). The sample synthesis process involved making two 4 wt% particle suspensions in isopropyl myristate, one with

N20, one with H30, then combining them in a 4:1 ratio before adding the Milli-Q water phase.

The emulsion was white and rigid enough to be turned upside-down but it formed droplets during the miscibility tests, and was confirmed to be O/W. The stability of the emulsion was visibly lower, compared to the simultaneous dispersing of the particles, as there was a non-negligibly thick layer of phase separated water at the bottom The optical microscopy images once again show dark spots of possibly aggregated silica, and wrinkles in the continuous phase scattered around in the examined sample area, as shown in *Figure 17*. The same microscopy sample contained double emulsion regions as well.

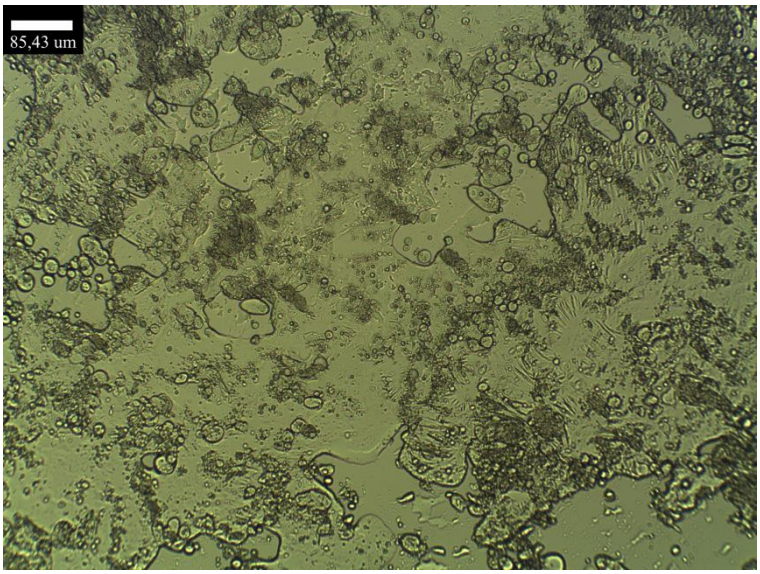

Figure 17: Micrograph of the 80% N20 and 20 % H30 silica containing emulsion, where 4-4 wt% N20 and H30 were dispersed in isopropyl myristate separately. The pH of the aqueous phase was set only by the silica particles. We can see dark spots of aggregates silica, most likely from H30 particles. The scale bar is 85,43 μm.

If a large portion of H30 particles are simply not dispersed in the sample, and are instead just aggregated in a “few” spots, then the majority of the sample could behave as if it was stabilized by only the hydrophilic N20 particles and create mostly O/W emulsions, as we have experienced. This would explain the emulsion type uncertainty up to 20-30% H30 silica content, because it can be up to “random chance” whether or not enough hydrophobic H30 particles are able to adsorb at the interface between the liquid phases of the emulsion and alter the mean curvature.

Dispersing H30 in water instead of isopropyl myristate does not help, because, as written earlier, a portion of the dry powder can float on the water surface, leading to losses in silica to the wall of the sample holder. This of course meant that we essentially had no control over the

silica amount nor the exact particle mixture in the emulsion system making samples nearly irreproducible. Setting the pH of the aqueous medium to 9,2 did not alleviate this issue due to the largely hindered adsorption of the charged silica aggregates.

Dispersing the silica mixture in isopropyl myristate and setting the pH of the aqueous phase to 10 was also tested. In this case we saw much less dark spots under the microscope and the average droplet diameter has increased from ca. 10 µm to 23 µm. This means that the dispersing of H30 particles was more successful if the pH of the aqueous phase was higher. The H30 particles were interacting with the aqueous phase during the ultra-turrax mixing, which is a lower energy process than the ultrasonication, but apparently this did help breaking up the larger aggregates and homogenizing the emulsion in respect to H30 to a certain extent, as seen in *Figure 18*. The increase in droplet sizes also suggests an increase in H30 fraction in the interfacial layers, as the mean curvature of the system was reduced compared to when the H30 particles were aggregated in large clusters.

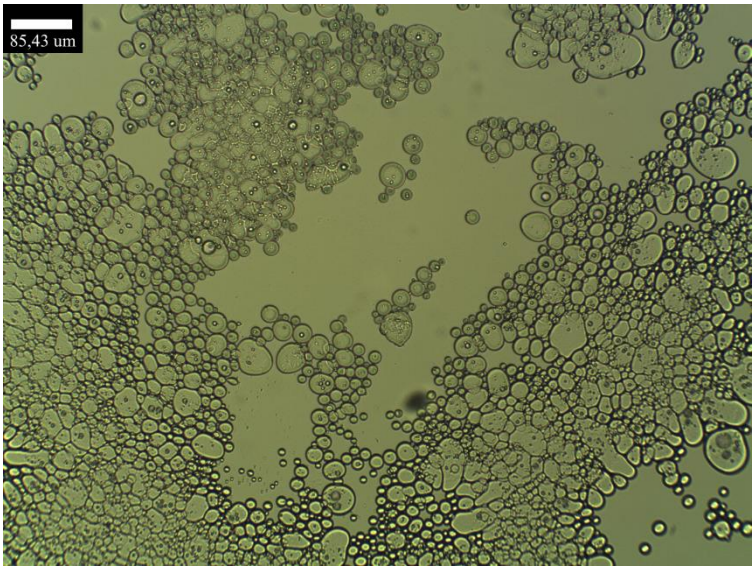

Figure 18: Micrograph of a 90% N20 and 10 % H30 silica containing emulsion, where the silica mixture was dispersed in isopropyl myristate and the pH of the aqueous phase was set to 10 initially. The H30 particles are not aggregated in large clusters and the droplet sizes also increased, compared to samples with pH control. The scale bar is 85,43 µm.

We can draw the conclusions that using a mixture of particles possessing different wettabilities can alter the interfacial curvature of an emulsion system, and that the pH of the aqueous phase can have great significance even if the particles are initially dispersed in another phase. The good dispersibility of the stabilizing particles is also an important factor in the homogeneous mixing of solid components in liquids and in modifying the net curvature of Pickering emulsions.

Silica Surface Charge Neutralization by CTAB Surfactant Adsorption

Although the composition of the silica mixture proved to be able to control the curvature of the isopropyl myristate – water interface, the inconsistency caused by H30 particles in the transitional phase inversion region was too great. We have instead shifted our focus to the *in-situ* hydrophobization of N20 particles. The adsorption of surfactant molecules alter the wettability of the particles due to the hydrophobic carbon chains. Since our target structure, a bijel, has a requirement of neutrally wetted particles[9], we saw an opportunity to achieve this with our relatively cheap commercially available silica nanopowders and CTAB surfactants. The preparation of CTAB coated silica particles could be a well-controllable, cheap, and quick process, with the additional benefit of gel formation slowing down the kinetics during emulsion structure formation.

We have made measurements at 0,1 wt% N20 concentration at pH ~ 9,2. Some level of partial sedimentation was observed at 1 CMC CTAB concentration. The turbidity of these samples was much lower than that of the 4 wt% N20 sols used in the previous section, but it is high enough to cause multiple scattering, meaning means that the graphs we present in *Figure 19* possibly show an unknown level of inaccuracy.

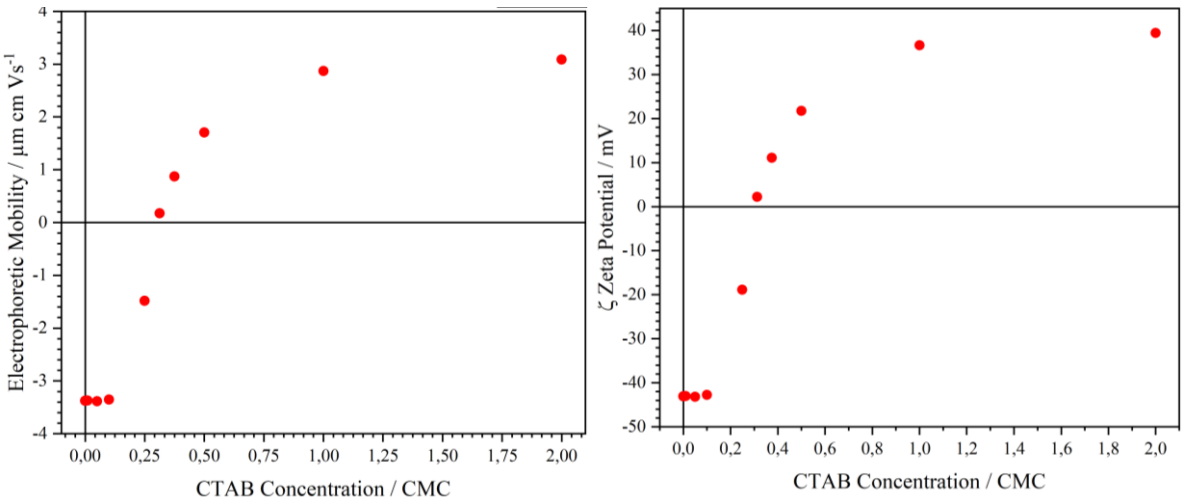

Figure 19: The measured electrophoretic mobility (left) and surface (zeta) potential (right) of 0,1 wt% N20 aqueous sol systems at pH 9. The size of the data points are about characteristic of the measurement errors.

This measurement was repeated for a series of samples with an increased N20 concentration of 1 wt% as well. The experiments were carried out in basic pH, ~ 9,2. We were expecting our dispersed silica nanopowder to undergo large scale aggregation and sedimentation, when the net surface charge density of the particle system neared zero. However, this did not occur,

instead, starting from 1 CMC CTAB and above the viscosity of the system has greatly increased. As an example for the degree of gelation, the air bubbles that were created upon injecting the sample back to the sample holder were still present after 2-3 weeks in the samples containing 1; 2; and 5 CMC CTAB, see *Figure 20*. This meant that the electrophoretic mobility measurements were no longer applicable since the particles motion was hindered by the increased viscosity and gel structure.

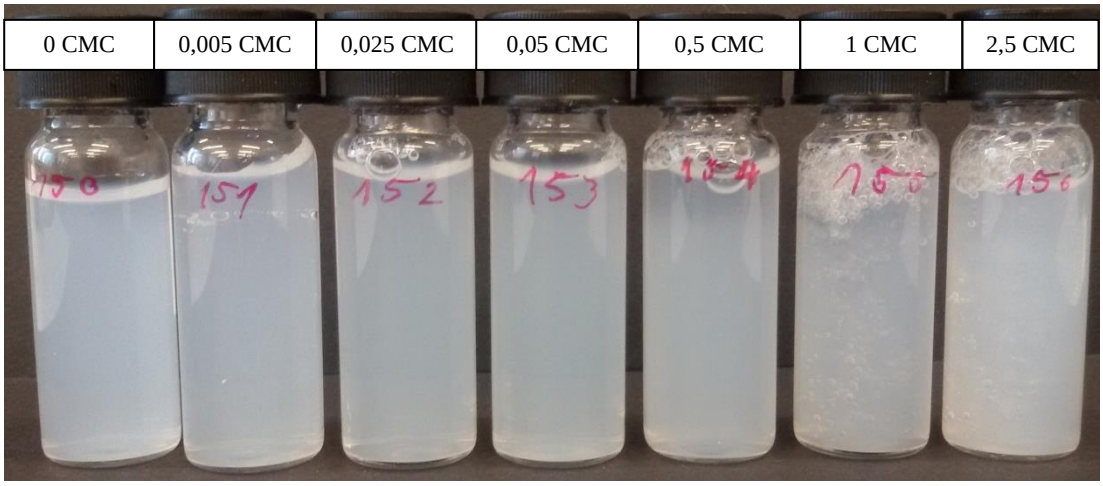

Figure 20: 1 wt% N20 particles dispersed in water with CTAB surfactant concentrations of 0; 0,01; 0,05; 0,1; 1; 2; and 5 CMC concentrations from left to right. All samples are at pH 9,2. From 1 CMC CTAB and above, the samples show gelation. (CMC = 0,92 mmol / dm^3)

Next we observed surfactant adsorption in the acidic pH (~ 5,3) the N20 particles set in the water. An experiment was performed, where we had only 0,2 wt% N20 with CTAB concentrations up to 0,15 CMC. The experiment was performed in an identical way to the experiments mentioned before. The results are shown in *Figure 21*, with the appearance of the samples as well. At this pH when the surface charge of the particles was near zero, large scale sedimentation has occurred, whereas at pH 9,2 it did not.

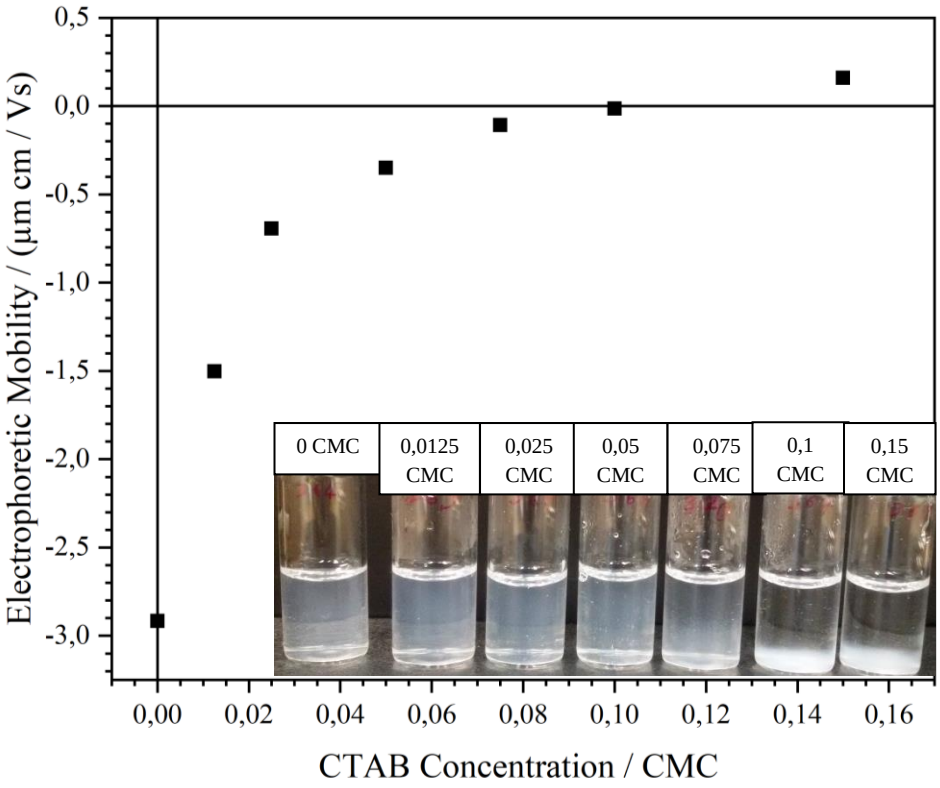

Figure 21: Electrophoretic mobility data and photo of the 0,2 wt% N20 containing aqueous suspensions in the presence of CTAB surfactants. At around 0,075 - 0,1 CMC the repulsion between particles is lowered to the point where macroscopic sedimentation can take place. The pH was set solely by the N20 particles.

The acidic pH experiment was repeated at 2 wt% N20 concentration as well, which decreased the pH down to 4,3. Although here the samples were one magnitude more acidic than in the previous case, the amount of CTAB required to achieve the same results increased by around one magnitude as well, meaning that the change in the N20 silica amount had a much more significant effect than the change in pH. The increased silica concentration was to better simulate emulsion conditions in later parts of the research. These samples have also shown a level of gelation at around 0,75 CMC CTAB, as some air bubbles remain in position and intact for a longer period of time. At higher CTAB concentrations, the viscosity of the samples decreases. It might be worth mentioning that this gelation takes place after the negative surface charges of the silica particles have been compensated or overcharged by the positively charged CTAB ionic surfactants.

The turbidity sharply increases at around 0,75 CMC CTAB concentration (about neutral surface charge), and then decreases back at higher CTAB concentrations. *Figure 22* shows the samples in increasing order of CTAB concentration, and the differences in their turbidity can be seen.

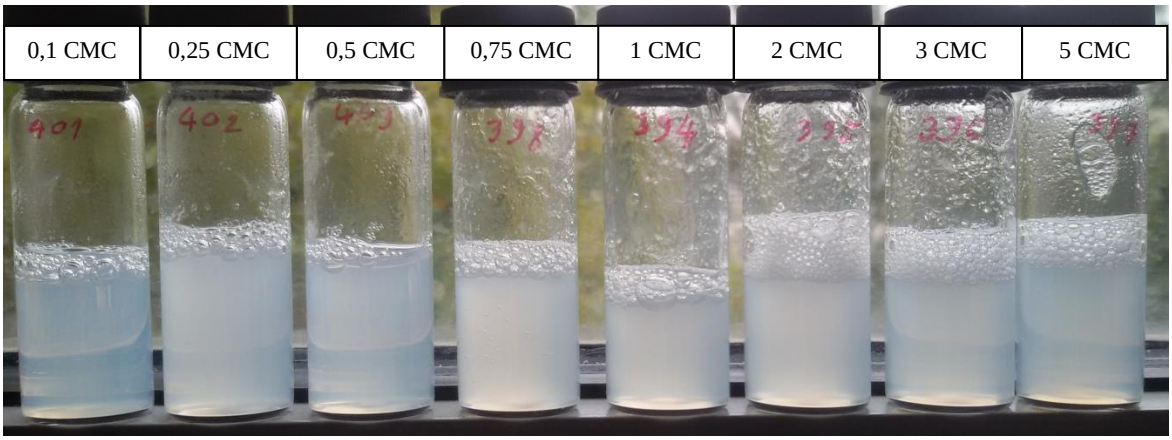

Figure 22: Photo of the 2 wt% N20 containing aqueous suspensions in the presence of CTAB surfactants. Although the background is not uniform, this picture shows the difference in absorbance the best. These were at pH 4,3.

These observations have shown that the N20 particles can undergo gelling at basic pH if 0,75-1 CMC CTAB is present to neutralize / overcharge their surface charges. At acidic pH however gelation is much less pronounced. This knowledge can be used to have better control over the formation kinetics of the interfacial layer of particles in emulsion systems.

Emulsions stabilized by N20 silica particle – CTAB surfactant interactions

Our earlier experiments, have confirmed, that the N20 particles are slightly preferably wetted by the polar water phase, thus the interfaces curve towards the oil, creating oil droplets, thus O/W emulsions. However, despite N20 being advertised as a hydrophilic silica, it appears to be relatively well dispersible in isopropyl myristate. Our main goal was to change the wettability of the silica particles' surface through the adsorption of CTAB in order to induce transitional phase inversion. If that could be achieved, then we would have to find a way to possibly "freeze" the system when the net curvature of the interfaces is near, or at zero, to have a chance for bijel formation[1-3,6,7].

As mentioned previously, N20 can be dispersed in both the water and oil phases, and will greatly affect the resultant emulsion system, see *Figure 23* as an example. It was already known to us that the behaviour and wettability of particles in Pickering emulsions depend partially on their starting phase[22]. An experiment of ours has demonstrated this, when in one set of samples we dispersed the N20 particles in isopropyl myristate, and in a complementary sample set the particles were in water with the CTAB surfactants already present during ultrasonication. After that the other liquid phase has been added 1) CTAB solutions to the

particles in isopropyl myristate; or 2) isopropyl myristate to the particles dispersed in CTAB solutions. The main difference between the two sets of samples is the way the CTAB surfactant could interact electrostatically with the silica aggregates. In the first one, the N20 particles and CTAB surfactants only meet at the oil-water interface, whereas in the second set they meet in the bulk water phase, from where they migrate to the interface. Naturally they also differ in the wettability of the particles by themselves due their different starting phase. For this experiment, small concentrations of CTAB solutions were used to avoid the possible gelation of the system as discussed in the earlier section. The concentrations were 0,0125 CMC; 0,1CMC; and 0,2 CMC CTAB.

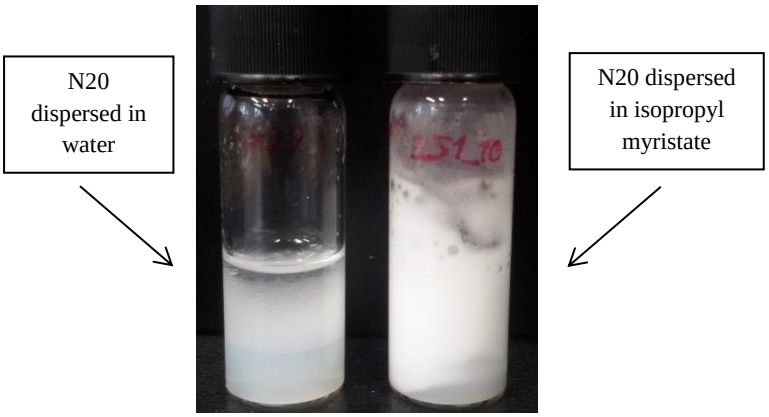

Figure 23: Photograph of 2 wt% N20 silica containing emulsions with the particles being dispersed in the water phase on the left, and in isopropyl myristate on the right. The two samples that have the exact same composition, are very different in most aspects. The pH was dependent solely on the N20 particles.

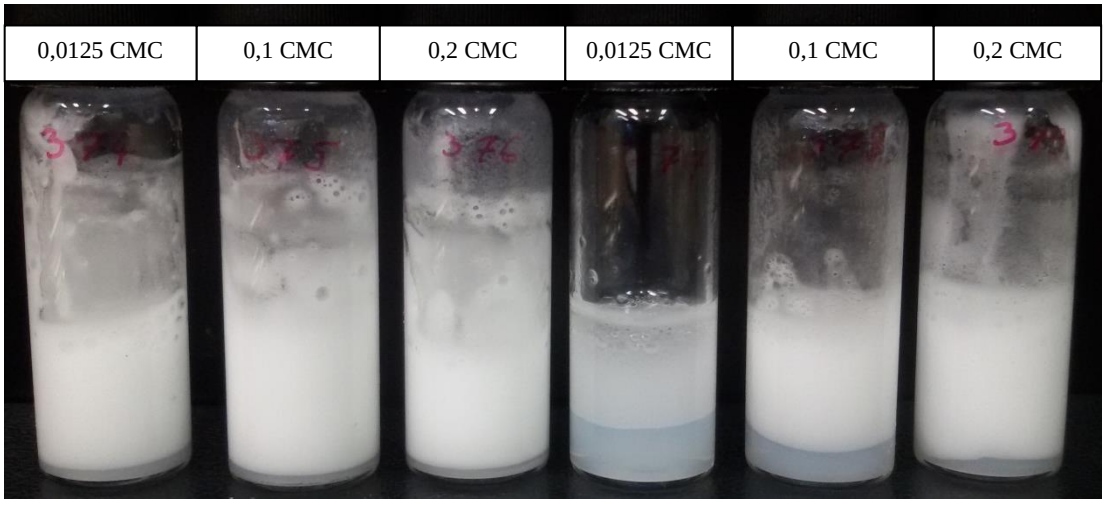

Figure 24: Photograph of 2 wt% N20 silica containing emulsions with the particles being dispersed in the isopropyl myristate phase on the left, and in water on the right. The sample sets are identical, save for the starting phase of the particles. The pH of the aqueous phase was set by the N20 particles to a minimum of 4,3 when dispersed in water initially.

The result of this experiment was quite spectacular, shown in *Figure 24*. The particles dispersed in isopropyl myristate led to much more stable emulsions. Some minimal amount of water may have been present beneath the emulsions, but most of the system was in the emulsion, and these samples remained stable for the next weeks. On the other hand, the particles first dispersed in CTAB solutions produced less stable emulsions, and had undergone visible phase separation in a few days, but they maintained some of the emulsion layer.

Optical microscopy shows a small decrease in droplet sizes as the surfactant concentration increases for both sample sets, an example is presented in *Figure 25*. No big aggregates of silica, irregularly shaped droplets, or wrinkles are observable, only spherical and slightly elliptical droplets are visible. The isopropyl myristate dispersed N20 particles could only interact with the CTAB surfactants in the L/L interface; therefore the surface modification of the particles was delayed and spatially restricted. On the other hand N20 particles dispersed in the aqueous CTAB solution were hydrophobized to a more significant degree, and this resulted in larger droplet sizes and no double emulsion forming.

A drop test was performed, where all emulsions remained droplets in isopropyl myristate, but they mixed with Milli-Q water. Both the results of the drop tests, and the appearances of the samples seen in *Figure 24*, lead us to conclude that the emulsions were of the O/W type.

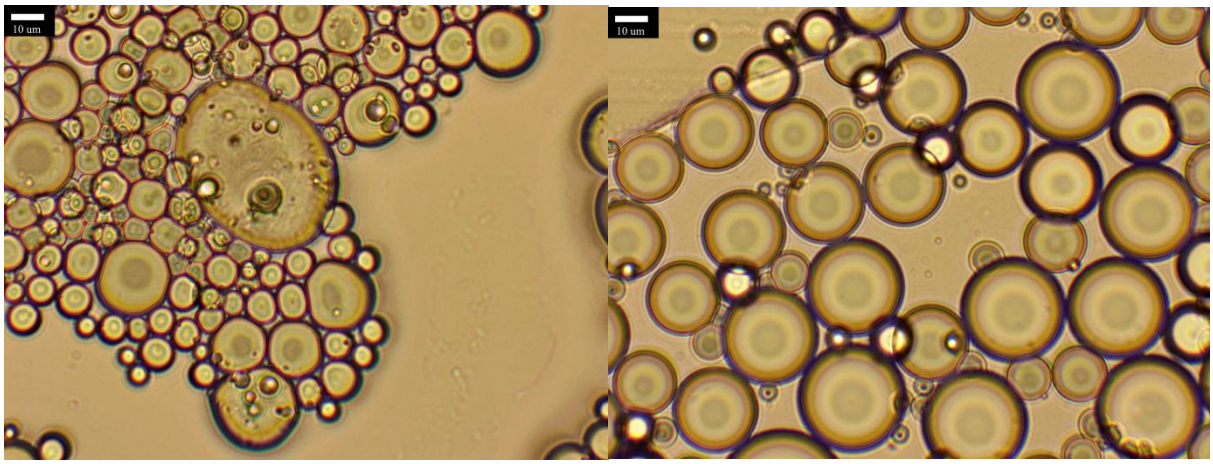

Figure 25: Micrographs of the emulsions containing 2 wt% N20 silica in the isopropyl myristate phase (left) and in the aqueous 0,1 CMC CTAB phase (right). Both samples contain 0,1 CMC CTAB in their water phase, the pH of which was acidic. The isopropyl myristate dispersed N20 could stabilize a W/O/W double emulsion with smaller droplet sizes, while the water dispersed N20 was immediately hydrophobized to some degree by the CTAB and stabilized an O/W emulsion with larger droplets.

Some of these samples have been exposed to air similarly to how we did with some of the solely N20 stabilized emulsions, to see if a similar structure would form. We have found that

during the drying of the 0,1 CMC CTAB containing sample, where the particles we dispersed in the water phase with the CTAB present, has formed a solid film on the droplet – air interface. This film was noticed because it showed signs of being torn on nearly every droplet of the dried area, and this film seemingly connected the droplets together. A micrograph is provided as an example on *Figure 26*. A few long and narrow channels are also visible between a few droplets; this was not an uncommon sight in these drying experiments.

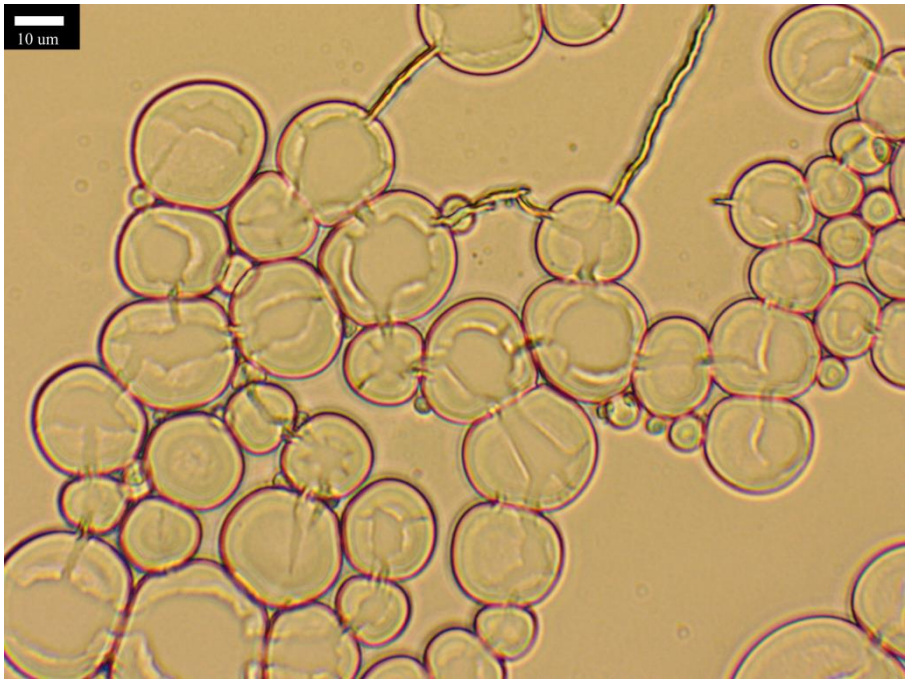

Figure 26: Micrograph of an emulsion containing 2 wt% total N20 silica and 0,1 CMC CTAB in the aqueous phase mixed with an equal volume of isopropyl myristate and let to dry in ambient air. The pH of the water phase was set only by the N20 particles. Aside from the long and narrow channels between a few droplets, a something like a solid film can be seen that shows marks of tearing on all droplets. The scale bar is 10 μm.

It is likely that the CTAB coated N20 particles create a solid film on the isopropyl myristate–air interface A possible reason of the ruptures in this film might be related to the appearance of capillary forces i.e. as the water evaporates between the N20 particles, they try to move closer together to reduce the contact area with the air, thus creating tension in the film.

Another experiment has involved dispersing 2 wt% N20 particles in isopropyl myristate, with 0,5; 1; 1,5; and 2 CMC CTAB concentrations in the water phase. This has been carried out without setting the pH of the water phases, so the 2 wt% N20 silica particles created an acidic environment (pH ~ 4,2). According to our electrophoretic mobility measurements, these CTAB concentrations are all in the concentration range where the 2 wt% total N20 particles are not overcharged. Therefore our expectation was due to the hydrophobization of

the silica particles, that the created emulsions would be W/O types. The particles coated only by a monolayer of CTAB would prefer being wetted by the isopropyl myristate, thus they would create a net curvature towards the water phase and creating water droplets in the oil phase. The appearance of the samples can be seen on *Figure 27.*

The droplet tests, however, suggested that at all investigated CTAB concentrations, the emulsion type remained O/W. The microscopy images, *Figure 28*, show a decrease in average droplet size in relation to the increase in CTAB concentration.

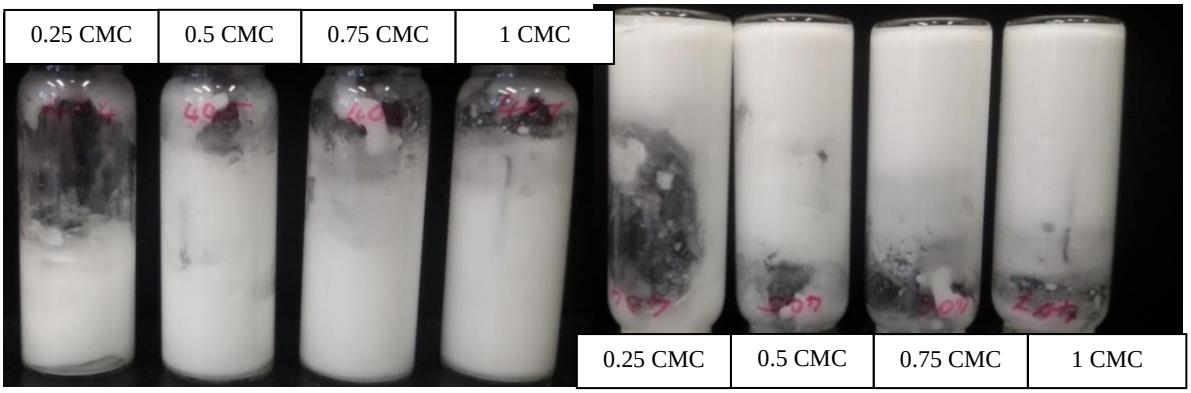

Figure 27: Photographs of 2 wt% N20 silica containing emulsions with 0,25; 0,5; 0,75; and 1 CMC CTAB concentrations. No phase inversion was observed despite our hypothesis. These experiments were carried out at pH 4,3.

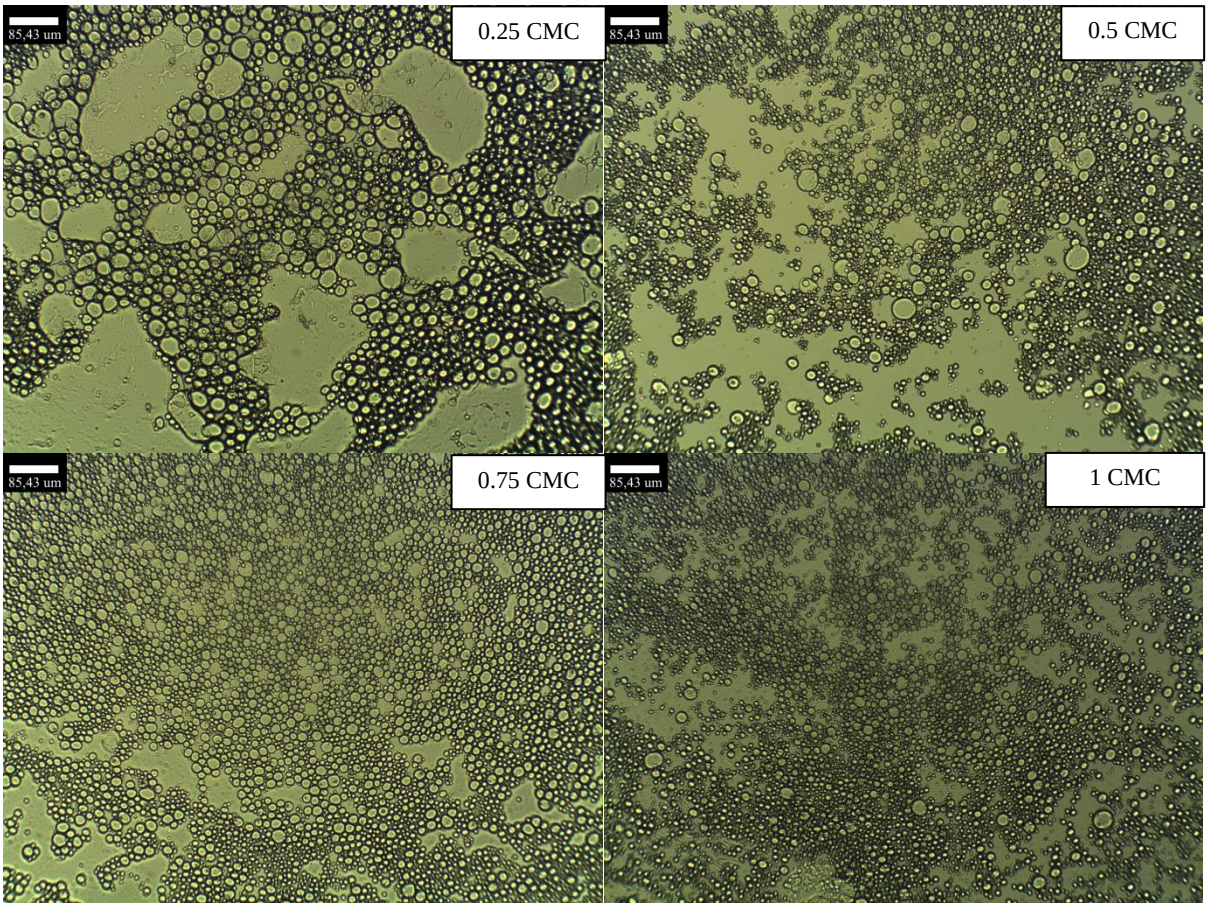

Figure 28: Micrographs of 2 wt% N20 silica containing emulsions with 0,25; 0,5; 0,75; and 1 CMC CTAB concentrations. These experiments were carried out at pH 4,3. A systematic decrease of average droplet diameters can be seen from ~ 21 μm at 0,25 CMC, to ~ 12 μm at 1 CMC. The scale bars are 85,43 μm.

Setting the pH between 9 and 10, the experiment has been repeated, with the 2 wt% silica nanoparticles being dispersed in isopropyl myristate; and in another set of samples, in the CTAB solution. We are discussing the samples that had the silica nanoparticles in the oil phase first. These samples contained 0,5; 0,75; 1; 1,5 CMC CTAB solutions at pH 10. This is the concentration range where the CTAB neutralizes the surface charge of the 2 wt% N20 particles and creates the most hydrophobic coating. The reason for using pH 10 CTAB solutions is that the silica particles at the interfaces can still protonate the water molecules and alter the pH. The extent of this effect is unknown to us, because the combined pH electrode can only give accurate values if the measured sample is oil-free, as pH itself is defined exclusively for aqueous phases. In an effort to balance this interfacial protonation, we decided to slightly increase the initial pH. As we have discussed previously, the difference in particle sizes and zeta potential at pH 9 and pH 10 is minimal.

2 wt% N20 silica would show a level of gelation at around the 0,75-1 CMC CTAB concentration interval at basic pH. However the silica particles were first dispersed in

isopropyl myristate in this experiment, which lowers the amount of particles that would be able to interact with the surfactants at the interface. The emulsions are white, solid gels that can be turned upside down without them falling. The results of the droplet tests suggested that all of the emulsion prepared this way are O/W in type. The microscopy images do not show silica aggregates, nor wrinkles in the continuous phase, only a decrease in droplet diameters. *Figure 29* provides examples of micrographs.

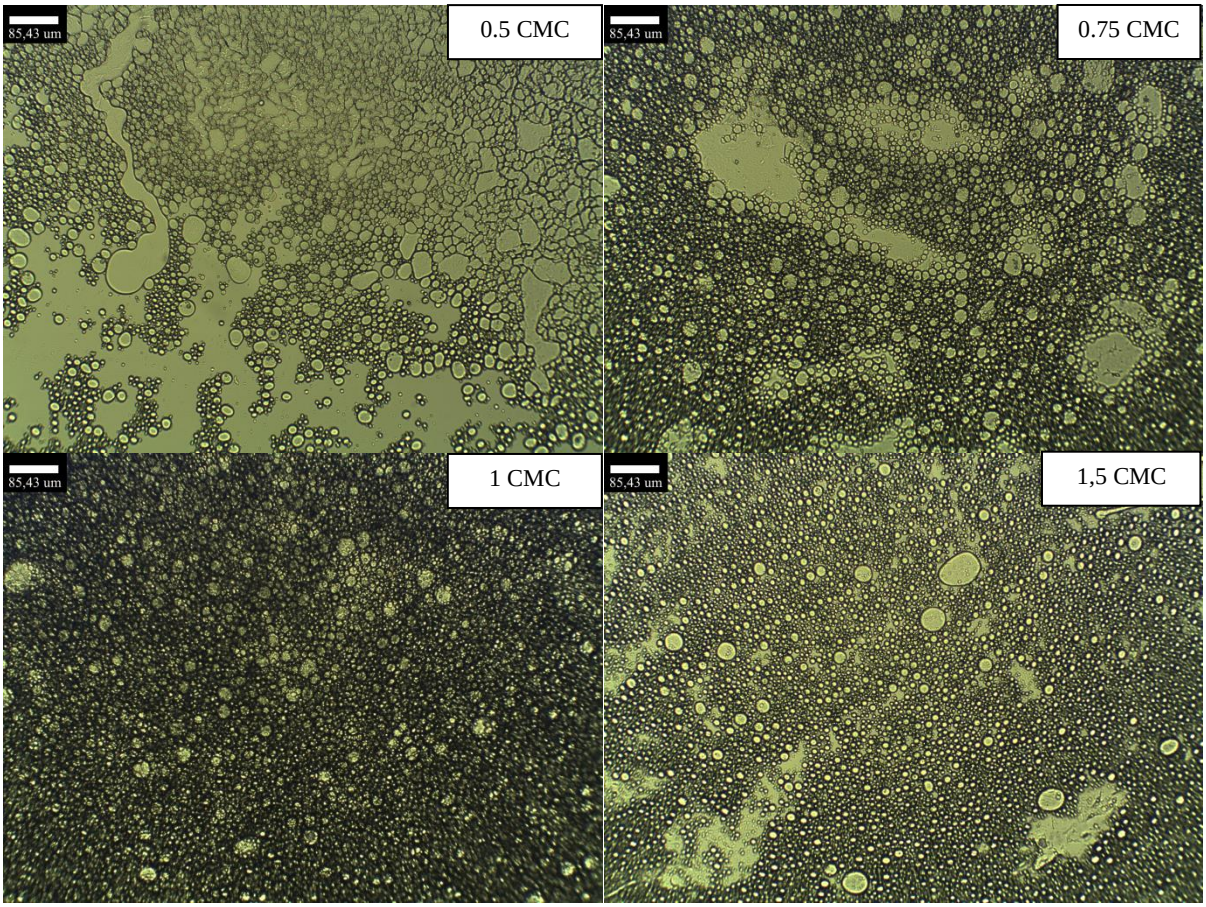

Figure 29: Micrographs of 2 wt% isopropyl myristate dispersed N20 silica containing emulsions with 0,5; 0,75; 1; and 1,5 CMC CTAB concentrations. These experiments were carried out at pH range of 9-10. A systematic decrease of average droplet diameters can be seen from ~ 18 µm at 0,5 CMC, to ~ 10 µm at 1,5 CMC. The scale bars are 85,43 µm.

The other sample set of this experiment contained the 2 wt% N20 silica nanoparticles in the aqueous phase with the same amounts of CTAB surfactants already present during the ultrasonic dispersing. The pH of the N20 particle dispersion were set to pH 9,2. Other than the pH setting method, every step of the sample creation process was identical. The emulsions were similarly white, and gel-like; and the droplet tests indicated that all of these samples were O/W type emulsions here as well. The micrographs *Figure 30*, are once again showing a decrease in droplet sizes in the function of increasing CTAB concentrations.

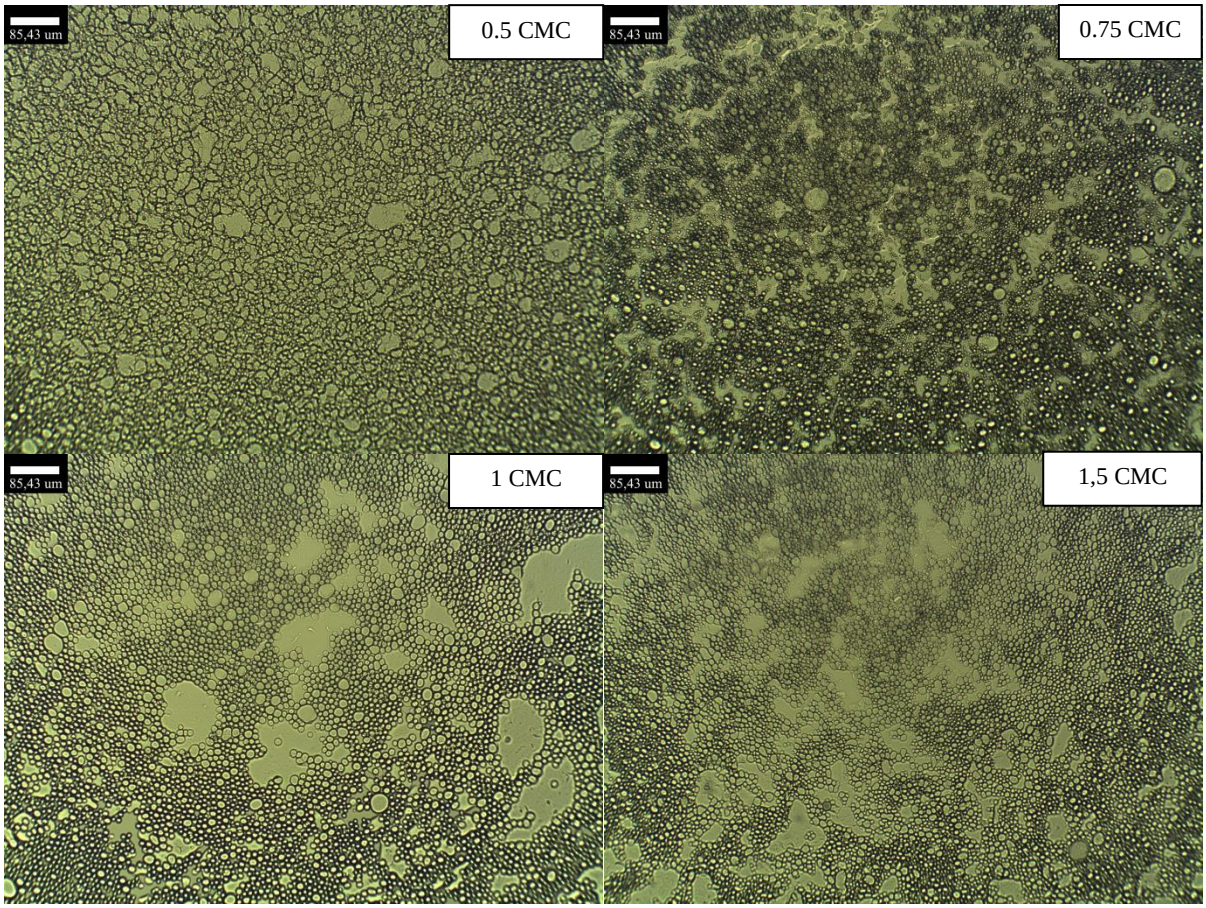

Figure 30: Micrographs of 2 wt% water dispersed N20 silica containing emulsions with 0,5; 0,75; 1; and 1,5 CMC CTAB concentrations. These experiments were carried out at pH 9,2. A systematic decrease of average droplet diameters can be seen from ~ 16 μm at 0,5 CMC, to ~ 7 μm at 1,5 CMC. The scale bars are 85,43 μm.

The final experiment we are discussing in this section is when we tried to repeat the previously described experiment at a wider CTAB concentration scale, and at two different pH levels. The goal was to give a final thorough examination of the produced emulsion types. This experiment has involved four sets of samples. The first one contained 2 wt% N20 particles dispersed in isopropyl myristate then pH 10 CTAB solutions were added to the samples. The water phases were 0,2; 0,75; 1; 1,5; 2; 3; and 4 CMC in CTAB concentration. The samples were again, white, hard-gels, see *Figure 31*, with most of the emulsion being attached to the glass wall of the sample holder, leaving air in the middle, where the ultraturrax mixing head was removed. All of the droplet tests yielded the same result, which was that all of these samples were O/W type emulsions. *Figure 32* shows micrographs of the 0,2 CMC and 4 CMC CTAB samples. It would appear that the CTAB does not increase the hydrophobicity of the N20 particles; rather it assists the N20 particles in stabilizing the O/W system. At 0,2 CMC CTAB the N20 particles' surface is still negatively charged with only partial CTAB coverage, and at 4 CMC the particles are overcharged with a surfactant double

layer. This double layer's surface has the surfactant hydrophilic head groups pointing outwards

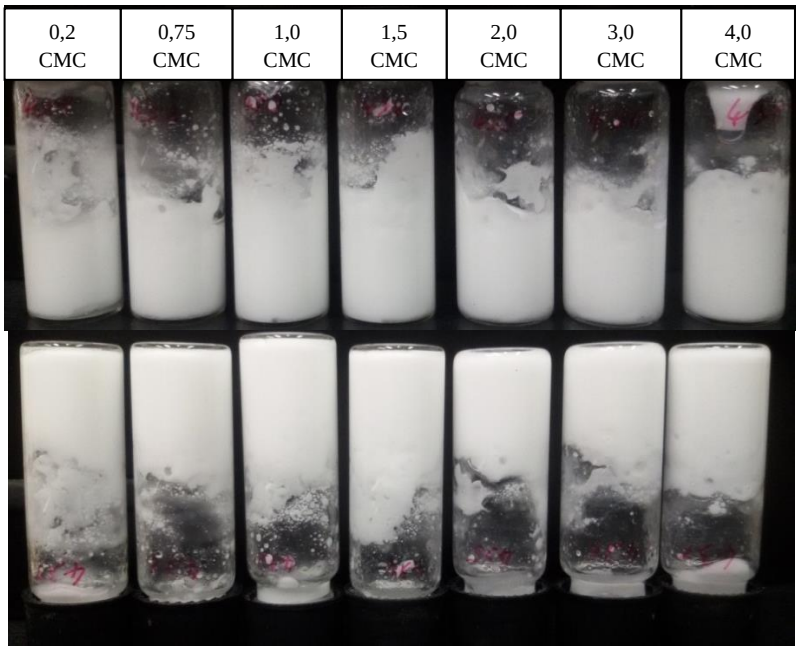

Figure 31: Photographs of 2 wt% N20 silica containing emulsions at 0,2; 0,75; 1; 1,5; 2; 3; and 4 CMC CTAB concentrations. The particles were dispersed in isopropyl myristate, and the water phase was set to pH 10.

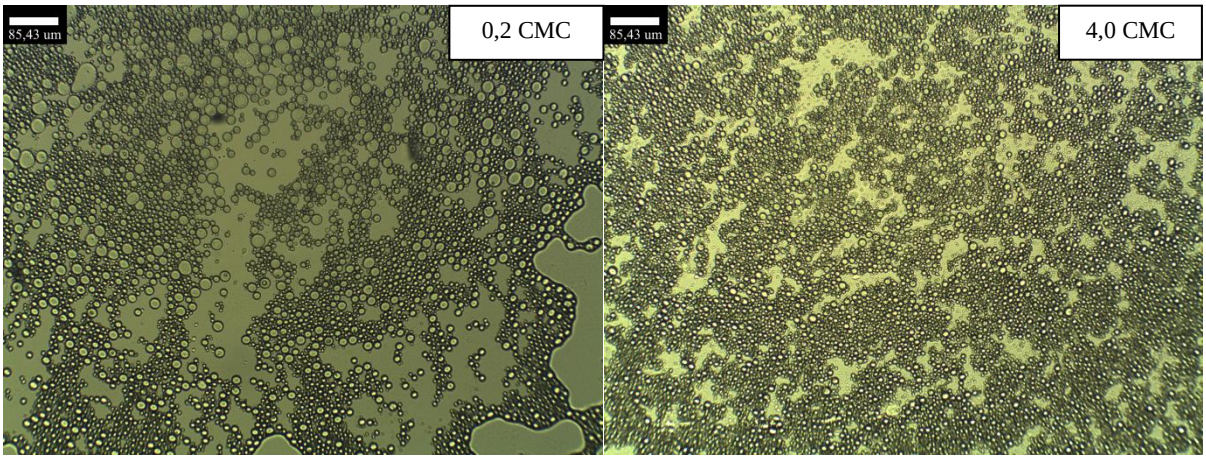

Figure 32: Micrographs of 2 wt% N20 silica containing emulsions at 0,2 CMC (left), and 4 CMC (right) CTAB concentrations. The particles were dispersed in isopropyl myristate, and the water phase was set to pH 10. We can see a decrease in droplet sizes as the CTAB concentration increases. This figure only shows the two endpoints in our experiment, but the change is gradual in-between.

This has been repeated without setting the pH of the CTAB solutions as well. These samples were created in an identical manner to the ones where the pH was set. These samples have also produced only O/W type emulsions, according to the droplet tests, and were similar in appearance. Their average droplet diameters under the microscope, *Figure 33*, were slightly smaller (~22 μm instead of 26 μm).

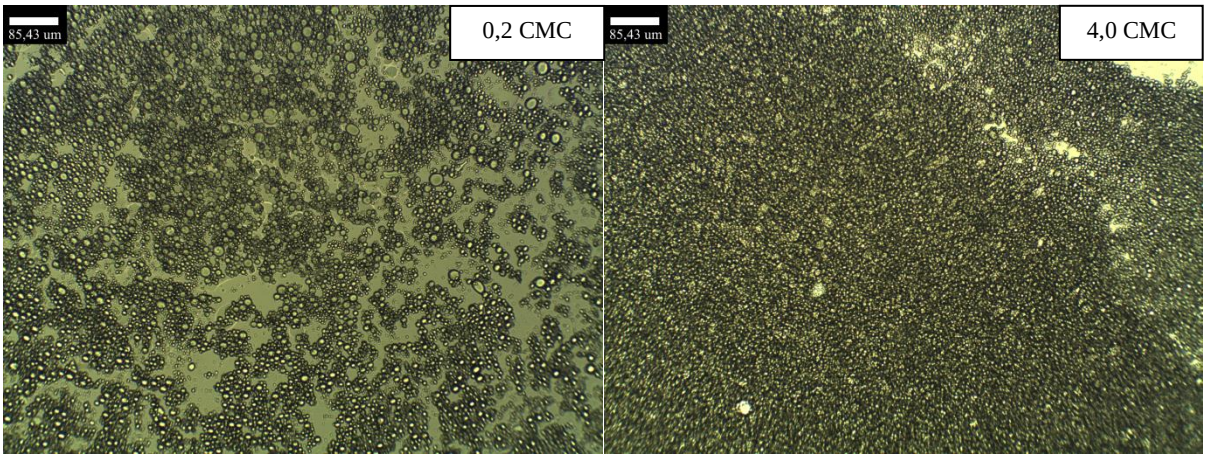

Figure 33: Micrographs of 2 wt% N20 silica containing emulsions at 0,2 CMC (left) and 4 CMC (right) CTAB concentrations. The particles were dispersed in isopropyl myristate, and the pH of the water phase was set to pH 9,2. We can see a decrease in droplet sizes and an increase in their density. These changes happened gradually as we increased the CTAB concentration.

Something that is worth mentioning that shortly after the ultrasonication, some of the N20 sols have formed hard gels, see *Figure 34*. The samples that have reached a viscosity to be turned upside down have 1,5 CMC or higher CTAB concentration, where the surface charge of the CTAB modified N20 particles is slightly above neutral.

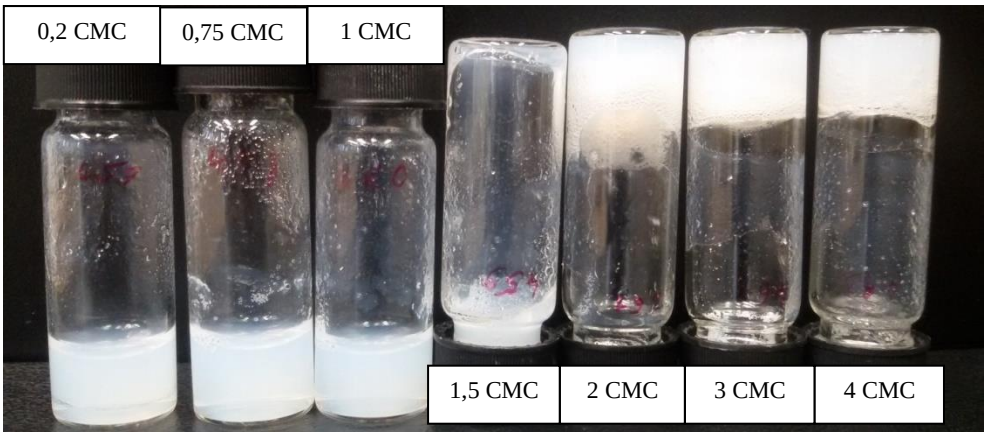

Figure 34: Photographs of 2 wt% N20 silica water suspensions just after ultrasonic dispersing at pH 9. Above a certain CTAB concentration the samples form gels within a couple of minutes.

The other two sample sets of this experiment were not pH controlled only the N20 particles determined the pH of the aqueous phase. Dispersing the particles in isopropyl myristate with CTAB on the other side of the interface yields larger droplets at lower pH compared to the previous higher pH observations. *Figure 35* shows the droplet sizes at 0,2 CMC and 4 CMC CTAB concentrations. The formed emulsions were similar macroscopically to the previously described experiment; the samples consisted of white gels that were smeared on the glass wall of the sample holders, and could be turned upside down. The droplet tests again suggested

that all emulsions were O/W. The average size of the droplets has decreased in the function of increasing CTAB concentrations.

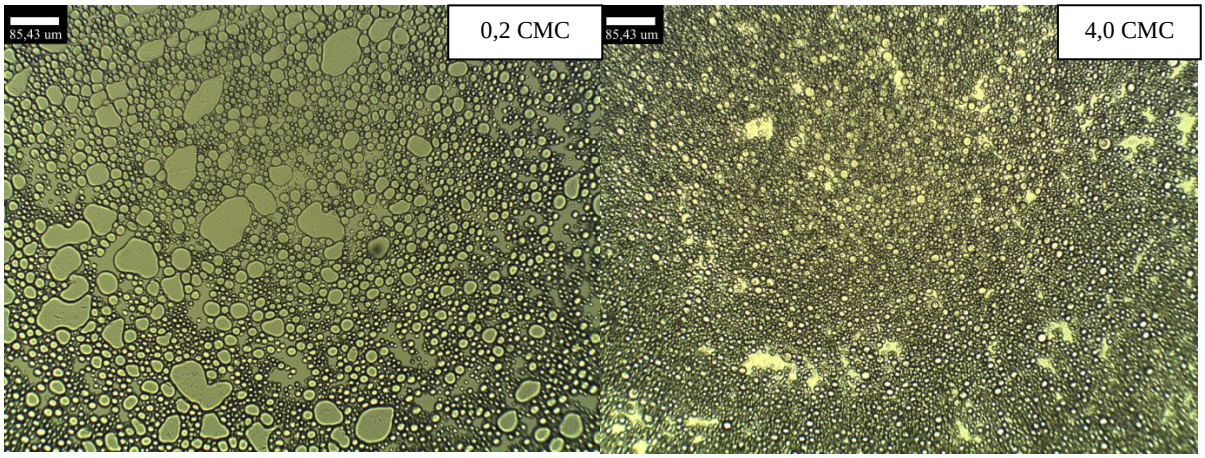

Figure 35: Micrographs of 2 wt% N20 silica containing emulsions at 0,2 CMC (left) and 4 CMC (right) CTAB concentrations. The particles were dispersed in isopropyl myristate, and the pH of the water phase was not set. The size of the droplets decrease, their circularity and packing density increase as the CTAB concentration increases.

Figure 36 shows the emulsions that formed when the particles were dispersed in the aqueous CTAB phase with no pH control. At 0,2 CMC CTAB large oil domains can be seen on *Figure 36*, which we believe is a result of the CTAB surfactant successfully increasing the hydrophobicity of the N20 particles. This effect is apparently only achievable at low surfactant concentrations, as going higher will increase the amount of surfactant adsorbed on the interface, which has an adverse effect on the interfacial curvature.

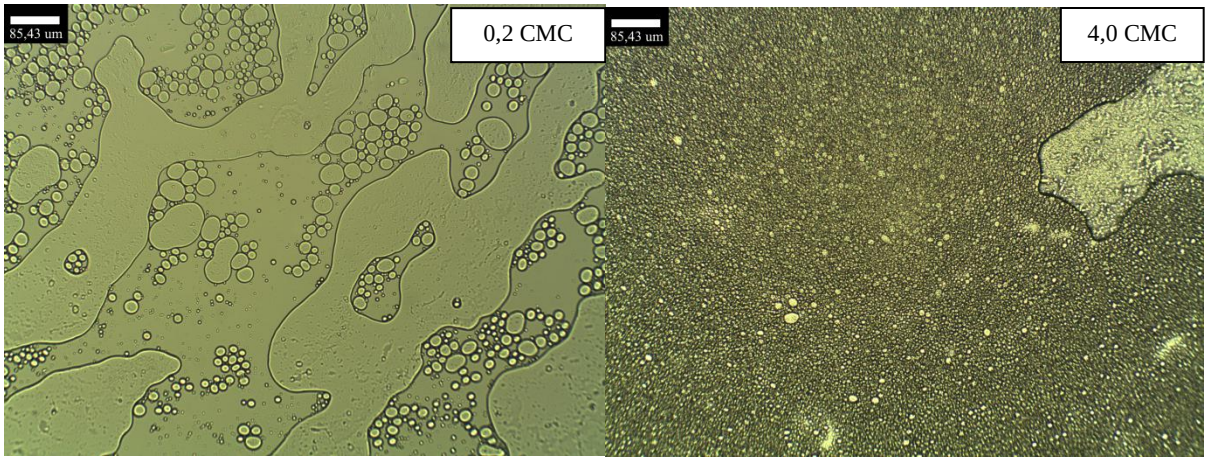

Figure 36: Micrographs of 2 wt% N20 silica containing emulsions at 0,2 CMC (left) and 4 CMC (right) CTAB concentrations. The particles were dispersed in the water phase the pH of which was not set. Here we can see large nearly continuous domains of isopropyl myristate along with droplets as well, instead of only droplets the pH was set to 9,2. We can also see this effect diminish at high surfactant concentrations.

In conclusion to this section, although preliminary experiments have confirmed the possibility of CTAB surfactants altering the wettability of N20 silica nanoparticles at low weight percentages, experiments to induce transitional phase inversion in emulsion systems stabilized by adequate amounts of nanoparticles are seemingly contradicting this hypothesis. It is possible to alter the wettability of N20 particles at lower surfactant concentrations; however this effect was not as significant as it would have been required. It is also worth noting that this effect was only really noticeable when the particles were dispersed in the water phase along with the CTAB surfactants, but not when the particles were dispersed separated from the surfactants. A possible reason could be that that CTAB could reversibly adsorb both at the isopropyl myristate/water and at silica/solvent interfaces dynamically modifying the wetting of the particles. However, this phenomenon needs further investigation.

Summary

Emulsion Structures From Commercially Available Silica Nanopowders

Dániel Hetey, MSc student in Material Science

Eötvös University, Budapest

Supervisor(s): **Dr. Róbert Mészáros**, University teacher
Institute of Chemistry, Eötvös Lóránd University

Emulsions are non-equilibrium, kinetically stabilized systems consisting of a continuous and a dispersed phase in the presence of a stabilizer. A new family of solid particle stabilized Pickering emulsions has been proposed then synthesised in the 2000s. The enormous interfacial area of this novel system is arrested by a semi-permeable monolayer of jammed, neutrally wetted colloidal particles. The good mechanical properties and the permeability of the particle monolayer arrested interface, coupled with the continuity of the liquid domains makes this system a promising template material for many applications.

The formation of such a structure is currently based on the quench-initiated spinodal decomposition of an initially homogeneous liquid mixture into two liquid phases, which is heavily limiting their potential compositions, macroscopic size and microscopic structure. The bijel literature contains very few publications discussing a new preparation method, and those that do are not very well explained, not receiving follow-up studies, leading us to the actual viability of the proposed methods. D. Cai, and P. S. Clegg et. al. have proven that a mixture of differently wetted particles can replace the special surface treated particles; and that the preparation of bijels is possible by simple mixing of two immiscible liquids replacing the spinodal phase separation. C. Huang et. al. have shown that one type of particle and a mixture of polyelectrolytes can also regulate the curvature of the interface. However currently none of these methods are exact science, further studies are needed.

Our work hypothesis was to induce transitional or catastrophic phase inversion under controlled experimental conditions since it guarantees the net zero curvature i.e. neutral wetting of the particles, giving a theoretical chance to their adsorption and jamming. In the first part of our work we have used hydrophilic N20 and hydrophobic H30 commercial silica particles to stabilize emulsions and induce transitional phase inversion. We used an environmentally-friendly and non-toxic apolar phase namely isopropyl myristate, and Milli-Q ultraclean water (pH 4,3, and 9,2) as the polar phase. N20 by itself has produced O/W or W/O/W double emulsions Furthermore, by letting some water quickly evaporate from a thin emulsion layer, a novel type of continuous, porous thin film of isopropyl myristate structure formed with domain sizes of 10s of micrometres.

H30 particles stabilized W/O emulsions by themselves, and were used as additives to N20 particles. N20-rich mixtures of them stabilized O/W and W/O emulsions with large uncertainty, attributed to the less than ideal dispersibility of H30 particles. Regardless, it proved that we can influence the interfacial curvature imposed by N20 particles by including small amounts of hydrophobic particles in the mixture.

In the second part of our work, CTAB surfactant was also used for *in situ* hydrophobization of our N20 particles in the hope of initiating phase inversion. At pH 9,2 and appropriately high silica concentrations, the CTAB coated N20 particles produced a loose gel network near and above charge neutralization CTAB concentrations. At pH 4,3 only the viscosity increased slightly, no gelation was observed.

Preparing emulsions with N20 dispersed in the isopropyl myristate phase and CTAB dissolved in water with or without adjusting the pH to 10, did not show significant change in the interfacial curvature compared to using pure water and no surfactants i.e. only O/W emulsions were detected. Not setting the pH of the aqueous surfactant solution had no relevant effect.

Preparing emulsions where the N20 particles were dispersed together with the CTAB surfactant in the aqueous phase led to much larger oil droplets, which indicates that the wetting of the particles has been altered. However, interestingly phase inversion could not be achieved in this case either. These results are probably attributable to the specific (nearly neutral) wetting features of the N20 particles at the isopropyl myristate - water interface.

Sources:

[1] Stratford, K. (2005). Colloidal Jamming at Interfaces: A Route to Fluid-Bicontinuous Gels. Science, 309 (5744), 2198–2201. DOI:10.1126/science.1116589.

[2] Herzig, E., White, K., Schofield, A. et al. Bicontinuous emulsions stabilized solely by colloidal particles. Nature Mater 6, 966–971 (2007). DOI: 10.1038/nmat2055

[3] Haase, M. F., Stebe, K. J., & Lee, D. (2015). Continuous Fabrication of Hierarchical and Asymmetric Bijel Microparticles, Fibers, and Membranes by Solvent Transfer-Induced Phase Separation (STRIPS). Advanced Materials, 27(44), 7065–7071. DOI:10.1002/adma.201503509

[4] Junzhi Li, Haoran Sun, and Min Wang Langmuir 2020 36 (48), 14644-14655 DOI: 10.1021/acs.langmuir.0c02507

[5] Mohraz, A. (2016). Interfacial routes to colloidal gelation. Current Opinion in Colloid & Interface Science, 25, 89–97. DOI: 10.1016/j.cocis.2016.07.005

[6] Cai, D., Clegg, P. S., Li, T., Rumble, K. A., & Tavacoli, J. W. (2017). Bijels formed by direct mixing. Soft Matter, 13(28), 4824–4829. DOI:10.1039/c7sm00897j

[7] Huang, C., Forth, J., Wang, W. et al. Bicontinuous structured liquids with sub-micrometre domains using nanoparticle surfactants. Nature Nanotech 12, 1060–1063 (2017). DOI: https://doi.org/10.1038/nnano.2017.182

[8] Bajpai, P. (2018). Colloid and Surface Chemistry. Biermann's Handbook of Pulp and Paper, 381–400. DOI:10.1016/b978-0-12-814238-7.00019-2

[9] Dr. Gilányi Tibor: Kolloidkémia – Nanorendszerek és határfelületek (egyetemi jegyzet) (http://www.chem.elte.hu/departments/kolloid/KolloidJegyzet_Ver1.0.pdf)

[10] Moroi, Y. (1992). Mixed Micelle Formation. In: Micelles. Springer, Boston, MA. DOI: https://doi.org/10.1007/978-1-4899-0700-4_10

[11] Kim, J., Lee, S., Choi, Y., Lee, S.-M., & Jeong, D. (2016). Basic Principles and Practical Applications of the Cahn–Hilliard Equation. Mathematical Problems in Engineering, 2016, 1–11. DOI:10.1155/2016/9532608

[12] B.P. Binks Current Opinion in Colloid & Interface Science 7 (2002) 21-41 DOI: 10.1016/S1359-0294(02)00008-0

[13] JOURNAL OF COLLOID AND INTERFACE SCIENCE 176, 378–387 (1995) DOI: 10.1006/jcis.1995.9954

[14] Clausse, M., Peyrelasse, J., Heil, J. et al. Bicontinuous structure zones in microemulsions. Nature 293, 636–638 (1981). DOI: https://doi.org/10.1038/293636a0

[15] Kunitake, M., Sakata, K., & Nishimi, T. (2012). Mesostructured Polymer Materials Based on Bicontinuous Microemulsions. Microemulsions - An Introduction to Properties and Applications. DOI: 10.5772/38642

[16] Gibaud, S., & Attivi, D. (2012). Microemulsions for oral administration and their therapeutic applications. Expert Opinion on Drug Delivery, 9(8), 937–951. DOI: 10.1517/17425247.2012.694865

[17] Toktam Farjami, Ashkan Madadlou, Trends in Food Science & Technology, 2019, 86, 85-94

[18] Cai, D., & Clegg, P. S. (2015). Stabilizing bijels using a mixture of fumed silica nanoparticles. Chemical Communications, 51(95), 16984–16987. DOI:10.1039/c5cc07346d

[19] Binks, B. P., & Lumsdon, S. O. (2000). Influence of Particle Wettability on the Type and Stability of Surfactant-Free Emulsions. Langmuir, 16(23), 8622–8631. DOI:10.1021/la000189s

[20] Fabrication of Solvent Transfer-Induced Phase Separation Bijels with Mixtures of Hydrophilic and Hydrophobic Nanoparticles Giuseppe Di Vitantonio, Daeyeon Lee, and Kathleen J. Stebea, DOI: 10.1039/D0SM00071J

[21] Scriven, L. Equilibrium bicontinuous structure. Nature 263, 123–125 (1976). DOI: 10.1038/263123a0

[22] Binks, B. P., & Murakami, R. (2006). Phase inversion of particle-stabilized materials from foams to dry water. Nature Materials, 5(11), 865–869. DOI:10.1038/nmat1757

[23] Ricardo Lopez Esparza, Ma Ba, Elías Pérez: Importance of Molecular Interactions in Colloidal Dispersions, Advances in Condensed Matter Physics, 1687-8108, 2015, DOI: 10.1155/2015/683716

[24] Wen, Z., Fang, L., & He, Z. (2009). Effect of chemical enhancers on percutaneous absorption of daphnetin in isopropyl myristate vehicle across rat skin in vitro. Drug Delivery, 16(4), 214–223. DOI:10.1080/10717540902836715

[25] Iwashita, Y. (2020). Pickering–Ramsden emulsions stabilized with chemically and morphologically anisotropic particles. Current Opinion in Colloid & Interface Science. DOI:10.1016/j.cocis.2020.05.004

[26] Horinek, D. (2014). DLVO Theory. Encyclopedia of Applied Electrochemistry, 343–3 46. DOI: 10.1007/978-1-4419-6996-5_7

[27] Fam, S. Y., Chee, C. F., Yong, C. Y., Ho, K. L., Mariatulqabtiah, A. R., & Tan, W. S. (2020). Stealth Coating of Nanoparticles in Drug-Delivery Systems. Nanomaterials, 10(4), 787. DOI: 10.3390/nano10040787

[28] Su, H., Hurd Price, C.-A., Jing, L., Tian, Q., Liu, J., & Qian, K. (2019). Janus particles: Design, Preparation, and Biomedical Applications. Materials Today Bio, 100033. DOI:10.1016/j.mtbio.2019.100033

[29] Binks, B. P. Particles as surfactants—similarities and differences. Curr. Opin. Colloid Interface Sci. 7, 21–41 (2002). DOI: https://doi.org/10.1016/S1359-0294(02)00008-0

[30] Kralchevsky, P. A., Ivanov, I. B., Ananthapadmanabhan, K. P. & Lips, A. On the thermodynamics of particle-stabilized emulsions: Curvature effects and catastrophic phase inversion. Langmuir 21, 50–63 (2005) DOI: 10.1021/la047793d